Review

Modulatory Effects of Bioactive Phytoconstituents on the Amplitude and Gating Properties of Membrane Ion Channels

Sheng-Nan Wu *, Guglielmina Froldi, Ya-Jean Wang, Rasa Liutkevičienė

Posted Date: 4 March 2026

doi: 10.20944/preprints202603.0263.v1

Keywords: phytoconstituents; voltage-gated channels; ionic current; ion channel; natural products; gating kinetics

 doi:10.20944/preprints202603.0263.v1

Review

Modulatory Effects of Bioactive Phytoconstituents on the Amplitude and Gating Properties of Membrane Ion Channels

Sheng-Nan Wu [1,*], Guglielmina Froldi [2], Ya-Jean Wang [3] and Rasa Liutkevičienė [4,]

[1] Department of Research and Education, An Nan Hospital, China Medical University, No. 66, section 2, Changhe Road, An Nan District, Tainan 70965, Taiwan

[2] Department of Pharmaceutical and Pharmacological Sciences, University of Padova, Largo E, Meneghetti 2, Padova 35131, Italy;

[3] Department of Senior Service Industry Management, Minghsin University of Science and Technology, 1 Xinxing Road, Xinxfen Township, Hsinchu County 304001, Taiwan

[4] Laboratory of Ophthalmology, Institute of Neuroscience, Lithuanian University of Health Sciences, Kaunas, Lithuania

* Correspondence: 071320@tool.caaumed.org.tw

Abstract

This review provides a comprehensive overview of the modulatory actions of plant-derived constituents on membrane ion channels in various cell types. Among their diverse bioactivities, ion channel regulation—governing membrane excitability, signal transduction, and cellular homeostasis—has emerged as a critical mechanistic basis for their pharmacological effects. Twenty-four representative phytoconstituents are discussed and classified into five major categories based on their structural features: alkaloids, terpenoids, lignans and acetogenins, polyphenols, and other aromatic and conjugated compounds. Across these categories, the reviewed compounds exhibit distinct and often highly specific effects on the amplitude and gating kinetics of multiple ionic currents, including voltage-gated Na^+ currents (I_{Na}), delayed-rectifier K^+ currents ($I_{K(DR)}$), M-type K^+ currents ($I_{K(M)}$), hyperpolarization-activated cation currents (I_h), erg-mediated K^+ currents ($I_{K(erg)}$), inwardly rectifying K^+ currents, and Ca^{2+}-activated K^+ currents ($I_{K(Ca)}$). Alkaloids predominantly suppress voltage-gated K^+ currents, with notable exceptions such as aconitine, which alters the properties of both I_{Na} and $I_{K(DR)}$, thereby contributing to its proarrhythmic toxicity. Terpenoids, including cannabidiol, croton diterpenoids, lutein, thymol, and triptolide, exert multifaceted effects on $I_{K(M)}$, I_h, inwardly rectifying K^+ currents, and Ca^{2+}-activated K^+ channels. Lignans and acetogenins, such as gomisin A, honokiol, sesamin, and squamocin, primarily modulate I_{Na}, I_h, and $I_{K(Ca)}$, with several compounds demonstrating strong links between ion-channel modulation and anti-neoplastic or neuroprotective actions. Polyphenolic compounds, including curcumin, eugenol, resveratrol, gastrodigenin, gastrodin, and pterostilbene, display diverse ion-channel targeting profiles, influencing multiple Na^+ and K^+ channel subtypes. Other aromatic or conjugated compounds, such as isoplumbagin, plumbagin, and verteporfin, regulate $I_{K(erg)}$ and $I_{K(Ca)}$, potentially contributing to both therapeutic efficacy and adverse effects. Collectively, the compound-specific modulation of current amplitude and gating kinetics offers valuable mechanistic insight into the pharmacological and toxicological significance of plant-derived natural products, highlighting the functional role of ion channel evaluation in guiding their therapeutic development and ensuring safety assessment.

Keywords: phytoconstituents; voltage-gated channels; ionic current; ion channel; natural products; gating kinetics

1. Introduction

 doi:10.20944/preprints202603.0263.v1

Plant-derived natural products, often referred to as phytochemicals, are secondary metabolites that plants produce to protect themselves from environmental stress, pests, and diseases. These compounds provide humans with a vast repertoire of bioactive properties that may contribute to the prevention or treatment of a wide range of diseases and disorders [1–4]. Among these bioactive properties, their regulatory effects on ion channels in the cell membranes of different cell types have long been an important subject of academic research. This review paper examines 24 phytoconstituents derived from plant natural products. Based on their major structural features, these compounds are broadly classified into five main categories: alkaloids, terpenoids, lignans and acetogenins, polyphenols, and other aromatic and conjugated systems (**Figure 1**). We present a comprehensive overview of the currently recognized modulatory effects of these compounds on membrane ion channels across a broad range of mammalian cell types.

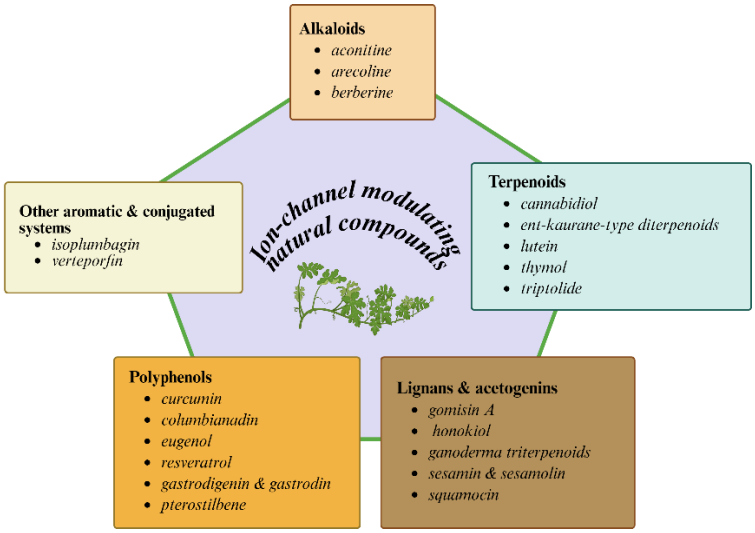

Figure 1. Graphic representation showing the five major categories of phytoconstituents and their potential modulation of ion channels. The five categories are alkaloids (pink), terpenoids (light blue), lignans and acetogenins (brown), polyphenols (orange), and other aromatic and conjugated systems (light yellow). Within each box, the phytochemicals discussed in this article are listed individually.

2. Alkaloids

2.1. Aconitine

Aconitine is an intensely poisonous alkaloid derived from plants of the genus *Aconitum* (Ranunculaceae) [5,6]. This compound is a proarrhythmic agent known to open tetrodotoxin-sensitive Na^+ channels in electrically excitable cells [7]. Aconitine-containing herbal extracts have also been reported to exert inhibitory effects on the proliferation of various neoplastic cells [6,8]. Studies have reported that this compound suppresses the delayed-rectifier K^+ current ($I_{K(DR)}$) in neurons, cardiomyocytes, and immune cells, leading to current inactivation upon membrane depolarization [9–13]. Recent findings indicate that aconitine can induce both early and delayed afterdepolarizations in neonatal cardiac cells and can trigger ventricular polymorphic tachycardia in rats [10,13]. These findings underscore the importance of understanding the electrophysiological impact of aconitine and similar compounds, considering their potential therapeutic applications and associated toxicities. Prior to evaluating the therapeutic potential of *Aconitum* extracts, such as their antitumor effects, it is essential to thoroughly assess the possible toxicities associated with these reagents.

2.2. Arecoline

 doi:10.20944/preprints202603.0263.v1

Areca nut (*Areca catechu*, family Arecaceae) has long been used as a medical and psychoactive stimulant in China [14] and a leading cause of oral cancer. Arecoline (1,2,5,6-tetrahydro-1-methyl-3-pyridinecarboxylic acid methyl ester) is an alkaloid extracted from areca nut and is a non-selective agonist of muscarinic receptors and that has been shown to have carcinogenicity, cytotoxicity and immunotoxicity [15,16].

The neuroprotective effects of arecoline were found in Alzheimer's disease [17]. It stimulates production of connective tissue growth factors in human buccal mucosal fibroblasts and induces the apoptosis of HaCaT keratinocytes [15,16]. An earlier report has demonstrated that in U373 and U87MG glioma cells, arecoline produces an inhibitory effect on intermediate-conductance Ca^{2+}-activated K^+ ($K_{Ca}3.1$-encoded, or KCNN4-encoded) channels in a concentration-, voltage- and state-dependent fashion [18]. The dissociation constant for arecoline-induced suppression of these channels was calculated to be 11.2 ◎M [18]. Arecoline-mediated membrane depolarization can arise primarily from its inhibition of intermediate-conductance Ca^{2+}-activated K^+ channels in these cells. Moreover, the major effect of arecoline on these channels is thought to be independent of binding to muscarinic receptor(s) [18]. Compounds like arecoline aimed block $K_{Ca}3.1$ channels could be tailored to become intriguing agents that potentiate the efficacy of other cytotoxic drugs for management of malignant gliomas or other types of neoplastic diseases [19].

2.3. Berberine

Berberine is an isoquinoline alkaloid found in many medicinal plants of the genera *Berberis* (Berberudaceae) and *Coptis* (Ranunculaceae). Preparations from these medicinal plants have been used as folk medicine in the treatment of jaundice, dysentery, hypertension, and other diseases [20]. Berberine alone was reported to possess anti-proliferative effects on human teratocarcinoma and hepatoma cells [21].

An earlier study reported that in human myeloma cells, berberine directly and differentially inhibits delayed-rectifier K^+ current ($I_{K(DR)}$) and Ca^{2+}-activated K^+ current ($I_{K(Ca)}$) in a concentration-dependent manner [22]. Berberine also effectively suppresses the proliferation of these cells. Because of the similarity between the potency and IC_{50} for blocking K^+ currents and inhibiting cell proliferation by berberine, the results suggest that inhibition of $I_{K(DR)}$ and $I_{K(Ca)}$ could be one of the mechanisms underlying berberine-induced anti-neoplastic actions [22]. In addition to its suppression of ion channels, berberine was reported to improve mitochondrial function and to increase apoptotic proteins, including cytochrome c, Bax, and caspase [23]. Therefore, berberine is a bioactive compound with potential for the treatment of various diseases, including glioma and Alzheimer's disease [24–26].

3. Terpenoids

3.1. Cannabidiol

Cannabidiol, which is considered a terpenophenol, is a non-psychoactive cannabinoid derived from the *Cannabis* plant (Cannabaceae), known for its potential therapeutic effects. It is among over 100 cannabinoids present in the plant and has been shown to be effective in treating various medical conditions, such as epilepsy, bipolar disorder, inflammation, and cancer [27]. Recent studies have demonstrated that cannabidiol influences the activity in the hypothalamic-pituitary-adrenal axis and modulates several ionic currents in excitable cells, including voltage-gated Na^+ currents (I_{Na}), M-type K^+ currents ($I_{K(M)}$), and hyperpolarization-activated cation currents (I_h) [28–30].

Cannabidiol exposure was noted to result in a concentration-dependent suppression of $I_{K(M)}$ in pituitary GH_3 lactotrophs, with an IC_{50} of 3.6 ◎M [30]. This compound also results in the suppression of I_h in the same cell type with an IC_{50} of 3.3 ◎M [30]. These findings suggest that the responsiveness of these ionic currents is complex and influenced by various factors, including the resting membrane potential, cannabidiol concentration, patterns of action potential firing, or combinations of these variables [30].

 doi:10.20944/preprints202603.0263.v1

3.2. Ent-Kaurane-Type Diterpenoids

The genus *Croton* (Euphorbiaceae) includes about 1300 species that are widely distributed throughout tropical regions. *C. tonkinensis* Gagnep., known as *Kho sam cho la* in Vietnamese, is a tropical shrub native to northern Vietnam and has been used commonly in Vietnam to treat different disorders [31]. *C. tonkinensis* is a rich source of diterpenoids [31], and its extracts were reported to exert anti-inflammatory and cancer chemopreventive activities [31,32].

Studies have shown that the fractions isolated from *C. tonkinensis*—specifically croton-01 (*ent*-18-acetoxy-7◎-hydroxykaur-16-en-15-one), croton-02 (*ent*-7◎,14◎-dihydroxykaur-16-en-15-one), and croton-03 (*ent*-1◎-acetoxy-7◎,14◎-dihydroxykaur-16-en-15-one)—are capable of modulating ionic currents in microglial SM826 cells, including the $I_{K(DR)}$ (encoded by Kv1.3) and the inwardly rectifying K^+ current (encoded by Kir2.1) [33]. The notable findings showed that in these microglial cells, croton-03 differentially suppresses Kv1.3- and Kir2.1-encoded currents in a concentration-, time-, and state-dependent manner. Voltage-dependent blocking by croton-03 of Kv1.3-encoded current with K_d (apparent affinity constant) and ◎ (fractional electrical distance) values of 5.17 ◎M and 0.091, respectively, was also estimated [33]. Therefore, the presence of these *ent*-kaurane diterpenoids is likely to disrupt cellular function by modulating the activity of these ionic currents.

Another report further demonstrated that the presence of croton-01, croton-02, and croton-03 produces concentration-dependent inhibition of I_h in pituitary tumor (GH_3) cells with effective IC_{50} values of 2.89, 6.25, and 2.84 ◎M, respectively [34]. Cell exposure to croton-03 was also noted to decrease the voltage-dependent hysteresis of this current in response to long-lasting isosceles triangular ramp pulse [34]. Therefore, croton derivatives and other structurally related *ent*-kaurane-type diterpenoids could represent intriguing compounds that use the open/activated state of the HCN channels as a substrate.

3.3. Lutein

Lutein (xanthophyll, ◎,◎-carotene-3,3′-diol), derived from a hydride of a (6R)-◎,◎-carotene, is one of the few xanthophyll carotenoids that is recognized to exist not only in vegetables and fruits, but also in high concentrations present in the macula of the human retina, where it is thought to act as a yellow filter [35,36]. A previous study showed that in pituitary GH_3 cells, the exposure to lutein is capable of suppressing hyperpolarization-activated cation current in a concentration-, state-, voltage-, and hysteresis-dependent manner [37]. A hyperpolarizing shift of the steady-state activation curve of hyperpolarization-activated cation current was also observed in the presence of lutein.

Furthermore, the subsequent addition of oxaliplatin or ivabradine, but still in the continued presence of 3 ◎M lutein, was capable of adjusting lutein-perturbed inhibition of I_h in GH_3 cells, as shown in **Figure 2**. Oxaliplatin or ivabradine has been shown to activate or suppress I_h, respectively [38–40]. Cyclic nucleotide-gated (CNG) channels (e.g., CNGA2 ion channels) were previously shown to exhibit hysteretic behavior of ion currents [41]. As shown in **Figure 3**, the experimental results disclosed the capability of I_h strength evoked by double ramp pulse to modify the varying patterns of bursting firing in different excitable cells, including central neurons [37,42].

 doi:10.20944/preprints202603.0263.v1

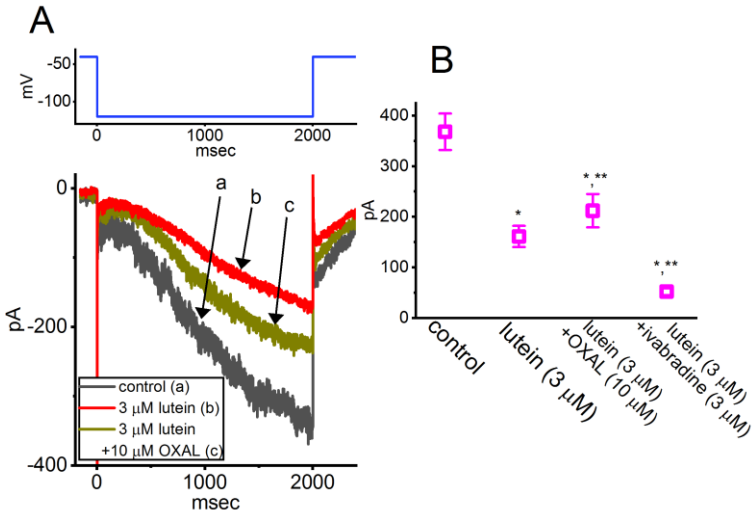

Figure 2. Comparisons among effects of lutein, lutein plus oxaliplatin (OXAL), and lutein plus ivabradine on the amplitude of hyperpolarization-activated cation current (I_h) recorded from pituitary GH$_3$ cells. In these experiments, whole-cell current recordings were performed in cells bathed in Ca^{2+}-free Tyrode's solution containing 1 ◎M tetrodotoxin, and during the measurements, the recording pipette was filled up with a K^+-enriched internal solution. **(A)** Superimposed I_h traces acquired in the control period (a, black) and during cell exposure to 3 ◎M lutein alone (b, red) or 3 ◎M lutein plus 10 ◎M oxaliplatin (OXAL) (c, brown). The upper part indicates the voltage protocol (blue) imposed on the tested cell. Of note, I_h exhibits slow activation in response to sustained hyperpolarization. **(B)** Summary scatter graph demonstrating the effect of lutein, lutein plus OXAL, and lutein plus ivabradine on I_h amplitude (mean ± SEM; n = 7 for each point). Each amplitude was measured at the end point of the 2-sec hyperpolarizing step from −40 to −120 mV. In the experiments on lutein plus OXAL or lutein plus ivabradine, lutein was first added to the bath before OXAL or ivabradine was further applied. * Significantly different from control ($p < 0.05$) and ** significantly different from the lutein alone (3 ◎M) group ($p < 0.05$). This figure is adapted from Ref. [37] and is published under the Creative Commons Attribution (CC BY) license.

In these current measurements, the tested cell was held at −40 mV and a long-lasting inverted double ramp pulse was applied [37]. The ramp pulse protocol comprises the downsloping (forward) ramp from −40 to −150 mV followed by the upsloping (backward) limb back to −40 mV, with a total duration of 3.2 sec (i.e., a ramp speed of ±69 mV/sec) as indicated in the upper part of **Figure 3A**. As demonstrated in **Figure 3**, the voltage-dependent hysteresis of I_h (i.e., the relationship of forward or backward I_h versus membrane potential) was observed upon activation by triangular double ramp pulse [43]. Notably, the I_h amplitude evoked by the downsloping phase of the inverted triangular ramp pulse was smaller (in absolute value) than that elicited by the upsloping phase, as indicated in the dashed arrows along the current trajectory (**Figure 3A**). For example, in the control (i.e., lutein was not present), the I_h amplitude at −120 mV taken during the downsloping or upsloping phase of double ramp pulse was markedly different ($p < 0.05$) (i.e., 48 ± 8 pA [downsloping] versus 249 ± 11 pA [upsloping], n = 7, $p < 0.05$). Under cell exposure to lutein (3 ◎M), I_h evoked in the downsloping limb of the inverted double ramp pulse was found to decline to a lesser extent than that measured from the upsloping end of the triangular ramp pulse. Moreover, the strength of lutein-induced current inhibition at the downsloping (forward) and upsloping (reverse) limbs of triangular ramp pulse differed significantly. As demonstrated in **Figure 3B**, the degree of I_h's hysteresis residing in GH$_3$ cells with or without the presence of lutein was further quantified. The results showed the effects of lutein and lutein plus ivabradine on the Δarea under the curve (i.e., the shaded region in **A**) [37]. For example, in addition to its depressive action on I_h magnitude, the addition of 3 μM lutein resulted in a reduction in the area responding to inverted triangular ramp pulse, as demonstrated by a reduction of Δarea from 17.7 ± 2.4 to 8.8 ± 1.6 mV·nA (n = 7, $p < 0.05$). After the lutein was removed,

 doi:10.20944/preprints202603.0263.v1

the hysteretic area returned to 17.2 ± 2.3 mV·nA. As cells were continually exposed to 3 μM lutein, subsequent application of 3 μM ivabradine measurably decreased the Δarea of voltage-dependent hysteresis further.

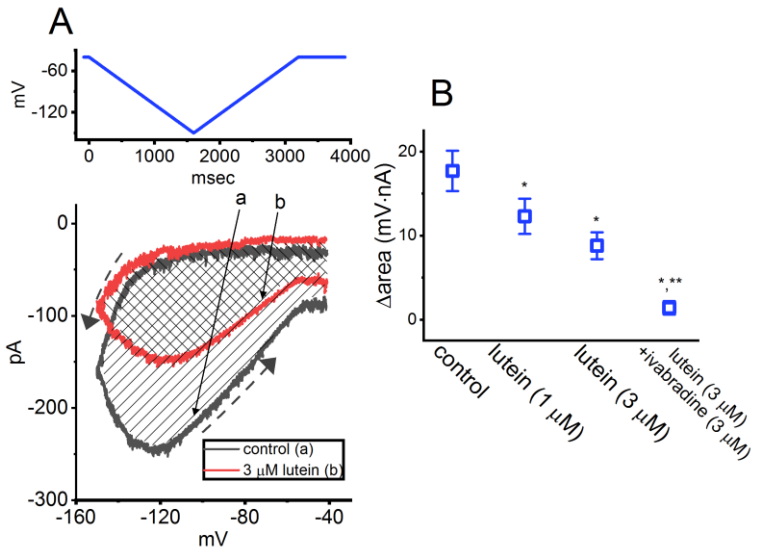

Figure 3. Modulation by lutein on the strength in voltage-dependent hysteresis of I_h recorded from GH$_3$ cells. **(A)** Representative current traces (i.e., the relationship of forward [descending] or reverse [ascending] current versus membrane potential) of I_h evoked by the inverted double (i.e., isosceles-triangular) ramp pulse (indicated in the top part, blue) in the absence (a, black) or presence of 3 ◎M lutein (b, red). The dashed black arrows along the current trace in the control period (i.e., lutein was not present) indicate an anti-clockwise direction of I_h trajectory in which time passes with the activated by inverted double ramp pulse, while the shaded region is the hysteretic area (◎area) with or without the lutein presence. Of note, I_h displays inward rectifying behavior together with voltage-dependent hysteresis. **(B)** Summary graph revealing effects of lutein (1 or 3 ◎M) and lutein (3 ◎M) plus ivabradine (3 ◎M) on the ◎area of voltage-dependent hysteresis. The ◎area refers to the shaded region under the I_h curve activated during the downsloping and upsloping limbs of triangular ramp pulse (mean ± SEM; n = 7 for each point). Notably, there was an emergence of ramp pulse-induced hysteresis for I_h elicitation, and the presence of lutein was concentration-dependently able to produce a measurable reduction in the ◎area of hysteretic current. ** Significantly different from control ($p < 0.05$) and * significantly different from lutein-alone (3 ◎M) group ($p < 0.05$). This figure is adapted from Ref. [37] and is published under the Creative Commons Attribution (CC BY) license.

The investigators further switched to current-clamp potential recordings in order to examine effects of lutein on sag potential in GH$_3$ cells [37]. Sag potential evoked in response to hyperpolarizing current stimulus has been shown to be closely linked to the presence of I_h in different types of excitable cells [43–46]. As shown in **Figure 4**, when the whole-cell potential recordings were achieved, a long-step 2-sec hyperpolarizing current injection with the amplitude of around 25 pA was noticed to induce the occurrence of sag potential (i.e., an abrupt drop-down to a lower level in the membrane potential upon hyperpolarizing current injection) [45]. Cell exposure to ivabradine (3 μM) was effective at suppressing the amplitude of sag potential. Furthermore, the application of 1 or 3 μM lutein resulted in a considerable depression of sag potential evoked in response to hyperpolarizing current stimulus [37]. Together, the findings can be interpreted to mean that, besides its antioxidative or anti-inflammatory properties [47], the existence of lutein can inhibit the amplitude as well as alter gating and hysteretic behavior of I_h, and that lutein's actions on ionic currents would engage in the modifications of spontaneous action potentials present in electrically excitable cells, presuming that similar in vivo observations occur [37].

 doi:10.20944/preprints202603.0263.v1

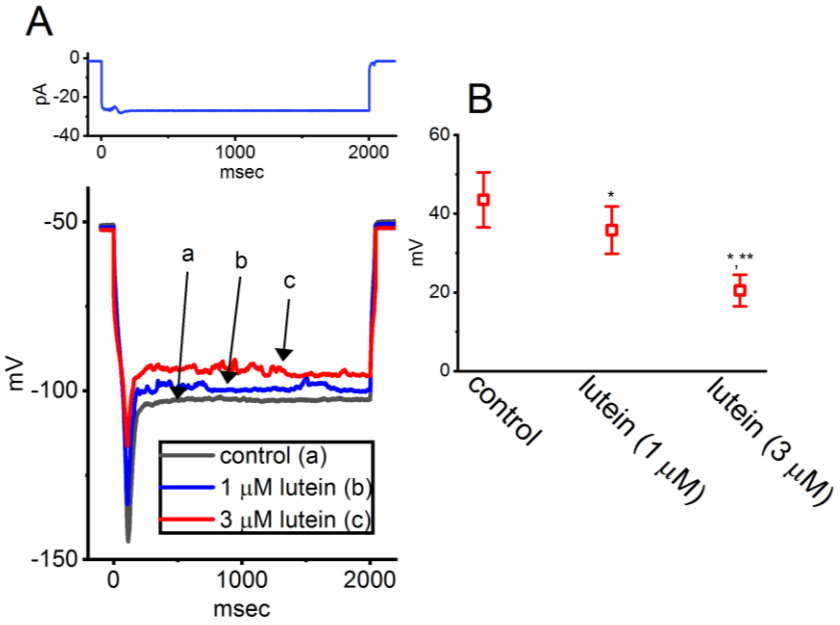

Figure 4. Effect of lutein on sag potential recorded from GH_3 cells. In these current-clamp potential recordings, cells were immersed in normal Tyrode's solution, which contained 1.8 mM $CaCl_2$ and 1 ◎M tetrodotoxin, and a long-lasting hyperpolarizing current stimulus with a duration of 2 sec was applied. **(A)** Representative potential traces acquired in the control period (a, black) and during cell exposure to 1 ◎M lutein (b, blue) or 3 ◎M lutein (c, red). The top part indicates the long-step current injection imposed over the tested cell. **(B)** Summary scatter graph showing the ability of lutein to alter the amplitude of sag potential (mean ± SEM; n = 7 for each point). Under the current-clamp configuration, the magnitude of sag potential (i.e., the difference between the start and end of hyperpolarizing current stimulus) was acquired with or without the presence of lutein. * Significantly different from control ($p < 0.05$) and ** significantly different from the lutein-alone (1 ◎M) group ($p < 0.05$). This figure is adapted from Ref. [37] and is published under the Creative Commons Attribution (CC BY) license.

3.4. Thymol

Thymol, a monoterpenoid phenol derived from thyme (*Thymus vulgaris*, Lamiaceae) essential oil, has been widely used as an antiseptic and antimicrobial agent [48–51]. Its aromatic properties make it a common ingredient in mouthwashes and dental preparations for treating oral infections [48]. Beyond oral care applications, thymol serves as a stabilizer in several therapeutic agents, including the anesthetic halothane, where accumulates in vaporizers during prolonged use. Notably, adverse effects following massive mouthwash ingestion have been attributed to thymol [52,53].

Previous studies have revealed that its biological activities may be partly mediated through modulation of ion channels. In particular, previous studies indicate that thymol influences Ca^{2+} signaling in pituitary GH_3 cells by enhancing capacitative Ca^{2+} entry and depleting intracellular Ca^{2+} stores, involving both thapsigargin–sensitive and thapsigargin–insensitive pools [54]. Moreover, thymol was reported to stimulate $I_{K(Ca)}$ in GH_3 cells [55]. These stimulatory effects on Ca^{2+} dynamics may contribute to the cellular mechanisms underlying the impact of thymol on neuroendocrine or endocrine functions.

3.5. Triptolide

Triptolide is a diterpene triepoxide isolated from traditional Chinese medicinal vine *Trypterygium wilfordii* Hook. F. (Celastraceae). It possesses multiple biological activities, including antitumor, immunosuppression, and antifertility effects [56]. Triptolide can protect neurons in the CNS and promote axon growth of dopaminergic neurons [57]. It also promotes spinal cord repair through down-regulation of astrogliosis and inflammation in an animal model of spinal cord injury

 doi:10.20944/preprints202603.0263.v1

[58]. This compound has been reported to inhibit proliferation and invasion of malignant glioma cells [59] and induce apoptotic cell death in malignant glioma cells [60]. Due to its small size and high lipid solubility, triptolide can cross the blood-brain barrier and produce significant effects on glial and glioma cells [56,60].

Previous studies showed that in human glioma cells (U373 cells), triptolide inhibits the inwardly rectifying K^+ current in a concentration-dependent manner with an IC_{50} of 0.72 ◎M [61]. Triptolide suppresses the activity of the inwardly rectifying K^+ channels in these cells with no change in single-channel conductance. The biophysical properties of the inwardly rectifying K^+ currents in U373 cells resemble the Kir4.1-encoded current because of positive mRNA detection of KCNJ10 (Kir4.1) and high sensitivity to inhibition by $BaCl_2$. KCNJ10, the gene that codes for Kir4.1, is recognized as a putative seizure susceptibility gene in mice and humans [62]. Therefore, the pharmacological actions of triptolide as described recently [56–60] could be partly, if not entirely, connected with its inhibition of the inwardly rectifying K^+ channels in glial or glioma cells. However, it should be noted that mRNA expression for other Kir channels may also occur in U373 cells.

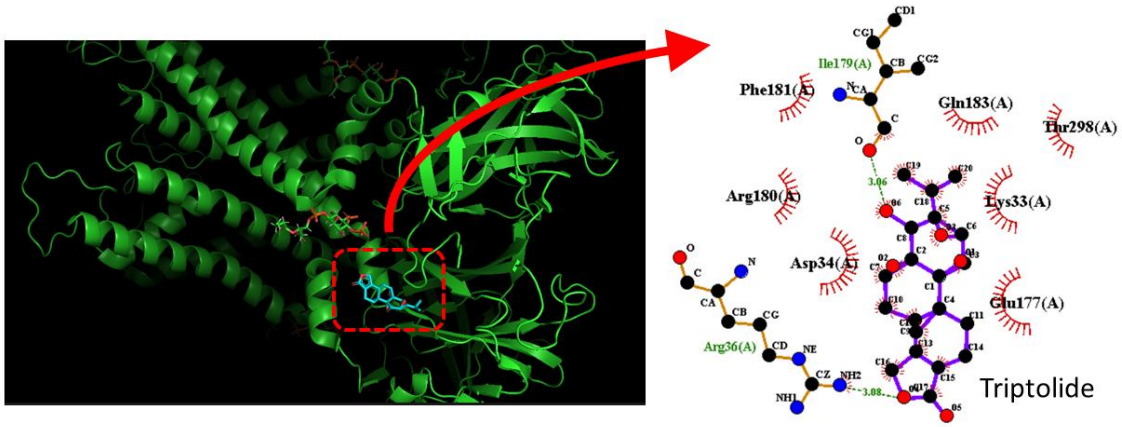

Figure 5. Docking interaction between the triptolide molecule and the KCNJ10 (or Kir4.1-encoded) channel. The left graph refers to the docking prediction between triptolide and the KCNJ10 channel. The protein structure of KCNJ10 was obtained from the Protein Data Bank (PDB ID: 815M), and the three-dimensional chemical structure of triptolide was retrieved from PubChem (Compound CID: 107985). On the left, the red dashed box highlights a snapshot of triptolide engaging hydrophobic interactions and forming hydrogen bonds with the channel, which is enlarged and illustrated on the right. The green dashed line indicates hydrogen bond formation, with bond lengths estimated at 3.06 and 3.08 Å. Of note, in this and the following figures showing predicted docking, the red arcs, with spokes pointing toward the triptolide molecule, denote hydrophobic contacts, and the corresponding graph in the right panel indicates an expanded display of red dashed box with a curve arrow in the left panel. .

We conducted a detailed analysis of the atomic interaction between the KCNJ10 protein [63] and triptolide using PyRx software, employing its embedded AutoDock function. **Figure 5** illustrates the predicted docking sites of the triptolide molecule. Notably, during the docking analysis with the KCNJ10 channel, triptolide was observed to form hydrogen bonds with residues Arg36(A) and Ile179(A), with bond lengths of 3.08 and 3.06 Å, respectively. Moreover, triptolide exhibited hydrophobic interactions with several residues, including Lys33(A), Asp34(A), Glu177(A), Arg180(A), Phe181(A), Gln183(A), and Thr198(A). These findings suggest a strong binding affinity between triptolide and the amino acid residues of the KCNJ10 channel, estimated at −7.8 kcal/mol. This interaction predominantly occurs within the intracellular domain of chain A in the KCNJ10 channel. This predicted interaction therefore raises the possibility that triptolide-mediated alterations in the magnitude and gating kinetics of the inwardly rectifying K^+ currents may occur independently of its binding to muscarinic receptors [61].

 doi:10.20944/preprints202603.0263.v1

4. Lignans and Acetogenins

4.1. Gomisin A

Gomisin A (wuweizichu B, wǔwèizi chún yǐ), a dietary dibenzocyclooctadiene lignan compound isolated from the hexane fraction obtained from the fruits of *Schisandra chinensis* (Schisandraceae) [64], has been reported to have anti-inflammatory, anti-oxidative, antihypertensive, neuroprotective, and anti-proliferative properties [65]. For example, this compound was previously reported to induce protective effects either against hepatic and renal injury induced by CCl_4 exposure, or nitropropionic acid-induced striatal toxicity, through differential regulation of the MAPK signal transduction pathway [66,67]. It could inhibit COX-2, iNOS, IL-6, TNF-◎ and NO· through the down-regulation of RIP2 and NF-◎B activation in mouse macrophages [68]. Earlier reports have also shown that gomisin A was able to exert antioxidative effects during osteoblast differentiation and in vascular endothelial cells [65,69], and to induce apoptotic changes in colon carcinoma HCT-116 cells [70]. Alternatively, the active components of *S. chinensis* were recently demonstrated to be detected after the intragastric administration of the lignans in rats [64]. The effectiveness of crude *S. chinensis* extract in decreasing prolactin production in pituitary GH_3 cells suggest that such extract could be therapeutically beneficial for patients with hyperprolactinemia and prolactinoma [71].

An interesting report demonstrated that the presence of gomisin A was able to produce an inhibitory action on I_{Na} in GH_3 cells in a concentration-, a time- and state-dependent manner. Cell exposure to gomisin A was also noticed to accentuate the inactivation rate of voltage-gated Na^+ current (I_{Na}), particularly at the slow component of current inactivation [72]. The inhibitory action on I_{Na} tended to be rapidly developing and readily washed out, and it would concurrently correlate in time with a significant rise in the inactivation rate of the current activated by short depolarizing pulse, while the activation kinetics of I_{Na} remained unchanged in the presence of gomisin A. In pituitary GH_3 cells, gomisin A differentially and effectively inhibited the transient or late components of I_{Na} with effective IC_{50} value of 6.2 or 0.73 ◎M, respectively [72]. The observed effect of gomisin A on the strength and gating of I_{Na} is primarily ascribed to this molecule acting largely on the voltage-gated Na^+ (Na_V) channel itself or its accessory subunits.

Next, the SCN9A ($Na_V1.7$) protein was docked with gomisin A using PyRx software. The predicted binding sites of gomisin A on this channel protein are illustrated in **Figure 6**. This compound establishes hydrophobic interactions with several residues, including Ser32(I), Ser820(B), Val821(B), Leu875(A), Phe876(A), Val914(A), Tyr915(A), Pro916(A), and Tyr917(A), which are located in the membrane-embedded segment of the channel. Since the results have shown an inhibitory effect of gomisin A on I_{Na} and a predicted interaction between SCN9A protein and gomisin A, this compound could potentially be applied to modulate the activity of $Na_V1.7$ channels in different cell types, thereby influencing their functional activity.

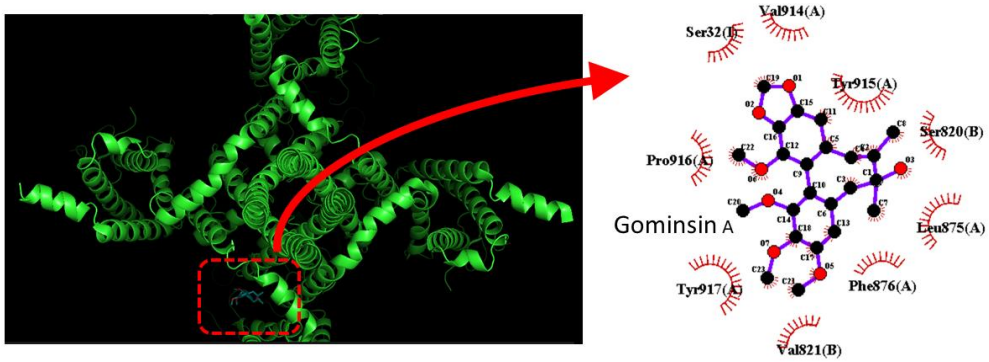

Figure 6. Docking result of $Na_V1.7$ (SCN9A) and gomisin A. The protein structure of SCN9A was obtained from PDB (PDB ID: 6N4Q) and the three-dimensional structure of gomisin A was from PubChem (Compound CID:

 doi:10.20944/preprints202603.0263.v1

15608605). The structure of SCN9A was optimally docked with gomisin A through PyRx in the red dashed box of the left side.

4.2. Honokiol

Honokiol, a hydroxylated biphenyl compound obtained from *Magnolia officinalis* and from other species (*Magnoliaceae)*, has been used in traditional Asian medicines (Houpo, Hou p'u, or Saiboku-to) [73]. Honokiol is recognized to be a potential natural compound that has been demonstrated to exert multiple effects on different cellular processes in various cancer models [74]. Previous studies have also revealed the effectiveness of this compound in modulating the functional activities of neuroendocrine or endocrine cells. For example, an earlier study has demonstrated that honokiol could induce cell cycle arrest and programmed cell death in vitro and in vivo in human thyroid neoplastic cells [75]. Several investigations have also reported the ability of *M. officinalis* bark or honokiol to modify the secretion of catecholamines from adrenal chromaffin cells [76]. Moreover, honokiol was noted to exert antidepressant effects by normalizing the hypothalamic-pituitary-adrenal axis [77].

Previous studies have demonstrated that the presence of honokiol produces concentration-dependent inhibition of I_h in GH_3 cells with an IC_{50} value of 2.1 ◎M (**Figure 7**) [78]. Honokiol shifts the steady-state activation curve of I_h toward a more negative potential with no modification in the gating charge of the current. This compound was able to attenuate the voltage-dependent hysteresis of I_h elicited by long-lasting triangular ramp pulse. It can also depress I_h amplitude in Rolf B1.T olfactory neurons [78]. The results unveiled the evidence that the honokiol presence is effective at inhibiting I_h in pituitary GH_3 cells and in Rolf B1.T olfactory neurons. The inhibition of these ionic currents was noted to be rapid in onset and is hence likely to be responsible for its modulatory action on functional activities in sensory neurons such as Rolf B1.T cells. Such inhibitory actions could lead to modifications in the firing behavior of electrically excitable cells, hence altering neuronal function [78].

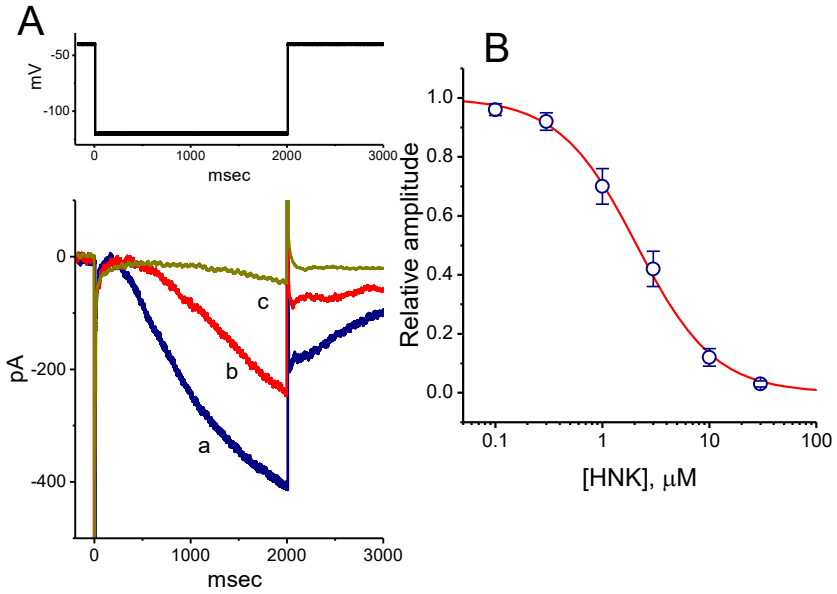

Figure 7. Concentration-dependent inhibition of hyperpolarization-activated cation current (I_h) by honokiol (HNK) in GH_3 cells. **(A)** Representative I_h traces obtained in the absence and presence of honokiol. In these experiments, we bathed cells in Ca^{2+}-free Tyrode's solution containing 1 ◎M tetrodotoxin, the recording electrode was filled with a K^+-containing solution, and the hyperpolarizing pulses from −40 to −120 mV were applied with a duration of 2 sec. Current trace labeled a is the control, and that labeled b or c was obtained after the addition of 3 ◎M honokiol or 10 ◎M honokiol, respectively. The upper part denotes the voltage-clamp protocol

 doi:10.20944/preprints202603.0263.v1

applied. **(B)** Concentration-response relationship for honokiol-induced inhibition of I_h (mean ± SEM; n=8 for each data point). The sigmoidal curve represents best fit to the Hill equation, and effective IC_{50} value was estimated to be 2.1 ◎M. This figure is adapted from Ref. [78] and is published under the Creative Commons Attribution (CC BY) license.

To examine how honokiol interacts with the HCN channel protein, we used the structure of HCN3 protein from PDB. The HCN3 channel protein structure was acquired from PDB (PDB ID: 8IO3), and PyRx software was used to see how the honokiol molecule docks into the channel protein. **Figure 8** presents the predicted docking sites of honokiol for interaction with amino-acid residues of the HCN3 channel. Specifically, the honokiol molecule was predicted to form hydrophobic contacts with residuals Phe60(D), Tyr89(D), Phe94(D), Ile237(D), and Phe238(D), as well as hydrogen bonds with residuals Ser90(D) and Asp91(D), with estimated distances of 2.95 and 3.10 Å, respectively. It is therefore anticipated that honokiol can interact with HCN channels to modulate the amplitude and gating kinetics of I_h [78].

Recent reports have demonstrated the ability of honokiol to exert antioxidant, anti-inflammatory, neurotrophic, and anti-apoptotic effects [79]. We also conducted a predicted docking analysis between honokiol and superoxide dismutase (SOD). SOD is a key antioxidant enzyme that plays a central role in controlling oxidative stress and modulating inflammation. We explored how SOD protein could be optimally docked with honokiol molecule by using PyRx software. The protein structure of SOD was obtained PDB (PDB ID: 1DO5). The predicted docking sites of the honokiol molecule with which the amino-acid residues can interact are presented in **Figure 9**. Notably, the honokiol molecule was predicted to form hydrophobic contacts with certain residues, including Asn142(B), Asn142(C), Ser143(B), Ser143(C), Gly145(C), Asn146(C), Ser233(A), Ala234(A), Gly235(A), and Leu236(A). The honokiol molecule was also predicted to form a hydrogen bond with residue Asp136(B) with a distance of 2.79 Å. These docking results suggest that honokiol can bind to SOD protein with a binding affinity of −7.4 kcal/mol.

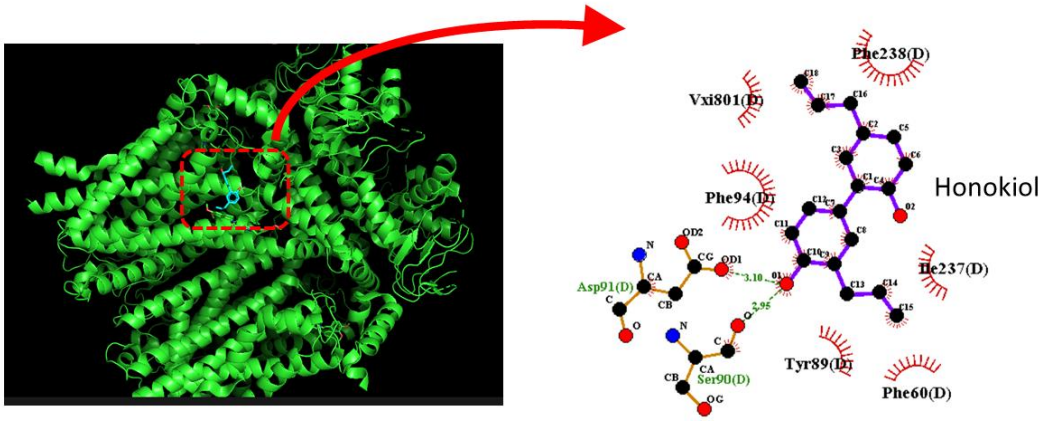

Figure 8. Predicted docking between the HCN3 channel and the honokiol molecule. The left panel depicts the HCN3-channel protein structure acquired from PDB (PDB ID: 8IO3), and the three-dimensional structure of honokiol from PubChem (Compound CID: 72303). PyRx software was used to show that the HCN3 channel structure can be optimally docked by the honokiol molecule. The right panel depicts an expansion of the red dashed box with an curved arrow in the left panel. This diagram of the interaction between the HCN3 channel and the honokiol was generated using LigPlot+.

 doi:10.20944/preprints202603.0263.v1

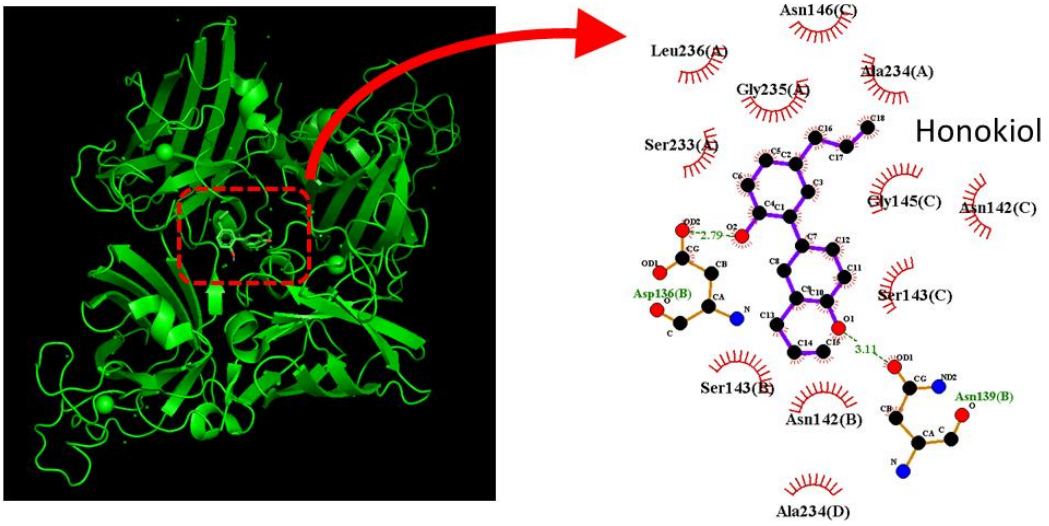

Figure 9. Molecular docking analysis of honokiol with superoxide dismutase. The protein structure of superoxide dismutase was acquired from PDB (PDB: 1DO5). The structure of superoxidase dismutase was docked with the honokiol molecule by using PyRx software, as indicated in the left side. The diagram of the interaction between superoxide peroxide protein and the honokiol molecule was generated by LigPlot+ (right side).

4.3. Ganoderma Triterpenoids

Ganoderma mushrooms (Língzhī in Chinese, or Reishi in Japanese) are a traditional Chinese herbal medicine that has been widely accepted as a nutritional supplement around the world. Among many species of the mushrooms, *Ganoderma lucidum* (Ganodermataceae) is most commonly used and it is commercially cultivated under controlled conditions to obtain mushrooms with more consistent chemical composition [80]. *G. lucidum* was reported to possess a variety of biological activities, such as antihypertensive, hypoglycemic, and hypocholesterolemic activities among other medicinal benefits [80,81]. The primary bioactive compounds were noted to include triterpenoids [81,82]. *G. lucitum* was also shown to prevent cardiac damage in animal models by alleviating the oxidative stress associated with myocardial injury [83].

Triterpenes are types of terpenes having a basic skeleton of C_{30} carbons. Triterpenoids have molecular weights ranging from 400 to 600 Da, and their chemical structure is complex and noted to be highly oxidized [84]. The triterpenoid fraction of *Ganoderma*, consisting of more than 300 lanostane triterpenoids, has been increasingly demonstrated to be effective at exerting biological actions, including providing effective antioxidant activities for prevention of myocardial injury, and producing neuroprotective actions [81,83,85]. *Ganoderma* triterpenoids could also suppress inflammatory response by directly scavenging the free radicals or systemically enhancing the antioxidant enzymes, thereby lowering lipid peroxidase in chicken livers or mice [83,85]. The aqueous extract was reported to exert anti-convulsant, anti-depressive, anxiolytic and anti-nociceptive actions [86].

Previous work has demonstrated that the inhibition by *Ganoderma* triterpenoids of I_h in GH_3 cells did not simply decrease current magnitude, but also altered the kinetics of the current, thereby indicating that they are able to produce a dose-, time- and state-dependent inhibition of I_h [87]. The steady-state activation curve of I_h in the presence of *Ganoderma* triterpenoids was shifted along the voltage axis toward the less depolarized potential. The IC_{50} value for *Ganoderma* triterpenoids-mediated inhibition of I_h observed in GH_3 cells (11.7 ◎g/mL) is comparable to concentrations reported for their antioxidative and neuroprotective effects [81,87]. Such intriguing actions could therefore be of pharmacological relevance and appear to be upstream of its effects on oxidative stress occurring inside the cell [80,81].

 doi:10.20944/preprints202603.0263.v1

4.4. Sesamin and Sesamolin

Sesame seeds and sesame oil obtained from *Sesamum indicum* (Pedaliaceae) have been recognized as health foods in Asian countries [88]. In comparison with other edible oils extracted from diverse seeds, sesame oil is extremely stable due possibly to the effective antioxidant activities presumably attributed to its abundance of lipid-soluble furofuran lignans such as sesamin and sesamolin [88].

Emerging research has demonstrated that sesamin and sesamolin, the two major furofuran lignans of sesame oil, exhibit multiple biological activities. These include suppression of lipid peroxidation in erythrocytes [89], inhibition of intestinal absorption of cholesterol and hepatic 3-hydroxy-3-methylglutaryl coenzyme-A (HMG-CoA) reductase activity [90], prevention of chemically induced mammary cancer, inhibition of ◎5-desaturase and chain elongation of C18 fatty acids, protection of hypoxic neuronal and PC12 cells by suppressing ROS generation and MAPK activation [91], as well as antihypertensive and cardioprotective effects [92].

Previous studies have shown that sesamin or sesamolin differentially and effectively inhibited the transient and late components of I_{Na} in a concentration-dependent manner in pituitary GH$_3$ cells [93]. The IC_{50} value of sesamin needed to lower the peak and the sustained I_{Na} were estimated to be 7.2 and 0.6 ◎M, respectively [93]. The addition of sesamin results in producing a modification of the inactivation kinetics of I_{Na} in response to brief depolarization. According to a Markovian model designed from the SCN8A channel adopted previously [93,94], sesamin-induced changes in the gating kinetics of Nav channel could be ascribed to its lowering of the probability of open (O) and open-blocked (OB) states of the channel. The results suggest that the inhibition by sesamin of these ion channels can be one of the ionic mechanisms underlying its remarkable changes in the functional activities of different types of electrically excitable cells, assuming that similar observations can be found in vivo [93]. Sesamin and other structurally similar compounds may serve as modulatory agents of Nav channels in neoplastic or neuroendocrine tumor cells within the field of cancer neuroscience, thereby suppressing tumor invasiveness and metastasis [95].

4.5. Squamocin

Squamocin is a bis-tetrahydrofuran acetogenin isolated from several genera of the plant family *Annonaceae*, including *Annona squamosa* (custard apple), *Annona muricata* (soursop), and *Asimina triloba* (pawpaw). Its structure is characterized by a long, alkyl chain bearing a terminal ◎,◎-unsaturated ◎-lactone ring, two tetrahydrofuran rings, and some oxygenated substituents along the chain. Squamocin is known to possess insecticidal properties [96] and anti-tumor effects [97]. Squamocin has been shown to inhibit the activity of mitochondrial NADH:ubiquinone oxidoreductase [98]. In addition, the cytotoxicity caused by asimicin, an analogue of squamocin, was thought to be associated with the regulation of membrane conformation [99]. It has recently been reported that squamocin could induce apoptosis in HL-60 leukemia cells and this effect was implicated in the activation of stress-activated protein kinase [100].

Previous studies reveal an interesting finding that squamocin produces a stimulatory effect on $I_{K(Ca)}$ in human coronary smooth muscle cells [101]. The stimulatory effect on $I_{K(Ca)}$ caused by squamocin was presumably related to changes in the level of intracellular Ca^{2+} concentrations. The results showing that the removal of extracellular Ca^{2+} inhibited the squamocin-induced increase in $I_{K(Ca)}$ amplitude, also suggest that both extracellular Ca^{2+} and internal Ca^{2+} release contribute to the increase in the current amplitude in these cells. It is likely that squamocin opens membrane ion channels with high Ca^{2+} permeability, can presumably account for its stimulatory effect on $I_{K(Ca)}$ [101]. The elucidation of the mechanisms by which the actions of squamocin and other structurally related compounds in different types of cells occur remains the aim of further research.

5. Polyphenols

5.1. Curcumin

 doi:10.20944/preprints202603.0263.v1

Curcumin (diferuloylmethane, 1*E*,6*E*-1,7-bis(4-hydroxy-3-methoxyphenyl)-1,6- heptadiene-3,5-dione), a major constituent of the spice turmeric obtained from *Curcuma longa* (Zingiberaceae), is a bright yellow diarylheptanoid produced by some plants. It is the principal curcuminoid of turmetic, which is a member of the ginger family (Zingiberaceae). This compound is largely used as a herbal supplement, cosmetics ingredient, food flavoring and food coloring [102]. Particularly, this nutraceutical compound has been demonstrated to possess beneficial properties in a variety of diseases ranging from cancer to diabetes mellitus [103]. For example, curcumin has been recently reported to influence insulin release from isolated pancreatic islets [104].

Curcumin has been reported to exert a concentration- and state-dependent depressant action on $I_{K(DR)}$ in pancreatic ⊚-cells, particularly in the rat insulinoma cell line INS-1 [105]. The inhibitory action on this K^+ current tends to correlate in time with a significant increase in the inactivation rate of the currents in response to membrane depolarization, while the activation kinetics of the current remained unaltered in the presence of curcumin [105].

The estimated peak of plasma curcumin concentration was previously reported to reach 3.14 ⊚g/mL (around 8.57 ⊚M) [106], a value which is apparently greater than the K_D (1.26 ⊚M) and IC_{50} (3.32 ⊚M) required for curcumin-mediated inhibition of $I_{K(DR)}$ seen in INS-1 cells [105]. Therefore, the inhibitory effects of curcumin and curcuminoids on these K^+ currents in pancreatic ⊚-cells are expected to occur at concentrations achievable in the human organisms, although whether the effects of curcumin and other curcuminoid derivatives on ionic currents in humans still remains to be further delineated.

5.2. Columbianadin

Columbianadin is one of the main bioactive constituents isolated from the underground part of *Angelica pubescens* Maxim. f. *biserrata* Shan et Yuan (Apiaceae) (*Angelicae Pubescentis Radix*, or "Duho [Dú huó]" in China). Columbianandin is a coumarin-type compound (an angular dihydrofuranocoumarin) which is recognized to have various biological activities that include analgesic, anti-inflammatory and anti-neoplastic effects [107,108]. This compound has been reported to induce changes in cellular proliferation or apoptosis [108]. It has also been previously demonstrated that carrageenan and lipopolysaccharide-induced inflammatory reaction are ameliorated by the application of columbianadin [107].

It is important to note that the presence of columbianadin could depress I_{Na} in a concentration-, time-, and state-dependent manner in GH_3 cells [109]. **T**his compound was found to differentially inhibit the peak and late amplitudes of I_{Na} activated by rapid membrane depolarization with effective IC_{50} values of 14.7 and 2.8 ⊚M, respectively [109]. It can shift the midpoint of the I_{Na} inactivation curve along the voltage axis to a more negative potential, despite its inability to alter the activation curve of the current. Subsequent addition of columbianadin was capable of depressing the tefluthrin-induced increase in the amplitude of persistent I_{Na} activated by the upright isosceles-triangular ramp at either upsloping or downsloping phase. Tefluthrin, a pyrethroid insecticide, can simulate I_{Na} [110–112]. In HL-1 cardiomyocytes, columbianadin was effective at depressing I_{Na} as well as at decreasing the slow component of the inactivation time constant of the current [109]. The experimental results suggest that columbianadin-mediated changes in the amplitude and gating kinetics of ionic currents tend to be upstream of its action either on cytosolic NOD1/NF-⊚B activation [113] or on the activity of antioxidant enzymes [114], and that they could conceivably participate in the adjustments of different functional activities in electrically excitable cells (e.g., GH_3 cells or HL-1 cardiomyocytes) occurring in vivo.

5.3. Eugenol

Eugenol (4-allyl-2-methoxyphenol) is an aromatic molecule found in several plants including clove (*Syzygium aromaticum*, Myrtaceae), bay leaves (*Laurus nobilis*, Lauraceae), and allspice (*Pimenta dioica*, Myrtaceae), and has been used in dental practice to relieve pain arising from a variety of sources, such as pulpal inflammations and dentin hypersensitivity [115]. Furthermore, eugenol is

 doi:10.20944/preprints202603.0263.v1

neuroprotective against excitotoxicity, cerebral ischemia and the toxic effects of amyloid-◎ peptides [116,117]. This compound has been demonstrated to suppress epileptiform field potentials and spreading depression in hippocampus and neocortex. These results suggest that the anti-convulsive properties of eugenol are mediated through the effects on neuronal ion fluxes by blocking Nav channels [118–120].

The evidence has emerged that the effects on ion channels may be an important mechanism underlying eugenol-induced actions in neurons. Previous studies demonstrated the ability of eugenol to bind to vanilloid receptors and, in turn, to activate non-selective cation channels [121]. A recent work has also reported that it produced an inhibition of voltage-gated Ca^{2+} current through Cav2.3 channels in the E52 cell line [122]. Such inhibition is thought to be direct and independent of the binding to vanilloid receptors or to ◎-adrenergic receptors [121,122].

Previous reports have demonstrated that the exposure to eugenol differentially inhibited the transient and late components of I_{Na} in differentiated NG108-15 neuronal cells in a concentration-dependent manner [123]. The IC_{50} values of eugenol required for the inhibition of the transient and late I_{Na} were 8.9 and 1.6 ◎M, respectively [123]. Eugenol can also diminish the amplitude of persistent I_{Na} evoked by long-lasting ramp pulse, and tefluthrin reversed the eugenol-induced inhibition of this current. This compound could decrease the frequency of spontaneous action potentials. It is therefore anticipated that the observed effects of this agent on ionic currents could be an important mechanism underlying its actions in neurons occurring in vivo [117,120,123].

5.4. Resveratrol

Resveratrol (trans-3,4′,5-trihydroxystilbene), a polyphenolic phytoalexin, is derived from various plants, including grape (*Vitis vinifera*, Vitaceae), peanuts (*Arachis hypogaea*, Fabaceae), and various berries. It has been demonstrated that resveratrol displays several pharmacological activities, including anti-platelet, anti-carcinogenic, anti-viral, and cardioprotective effects [124–126]. Moreover, there is accumulating evidence indicating that resveratrol exhibits neuroprotective effects [3,125,127]. In fact, resveratrol attenuates kainic acid-mediated convulsion and the associated neurotoxicity and also protects against pentylenetetrazol-induced seizure [128,129].

An important finding has reported that the suppressing effect of resveratrol in rat cortical neurons on action potential firing rate may be mediated by both stimulation of $I_{K(Ca)}$ and suppression of I_{Na} [130]. The increased amplitude of $I_{K(Ca)}$ is attributed to the stimulation of large-conductance Ca^{2+}-activated K^+ channels [124,130]. Inhibition of I_{Na} by resveratrol was reported to account for its analgesic effects [131]. With dual effects on $I_{K(Ca)}$ and I_{Na}, resveratrol might have the potential as a broad-spectrum anti-seizure medication.

5.5. Gastrodigenin and Gastrodin

Gastrodigenin (*p*-hydroxybenzyl alcohol, 4-hydroxybenzyl alcohol) is a phenolic compound found in the traditional Chinese herbal medicine *Gastrodia elata* Blume (Orchidaceae), which is commonly known as Tian Ma in Chinese or Chunma in Korean [132]. Gastrodin, the glucoside of gastrodigenin, is the major bioactive ingredient which can be isolated from *G. elata*. In East Asian countries, the dried rhizomes have been widely used for centuries to treat many neurological and psychiatric disorders, including convulsive disorders, dizziness, dementia, depression and migraines [133–136]. Increasing research is being conducted to determine the underlying molecular mechanisms through which the active constituents of *G. elata* may exert their pharmacological effects.

Previous studies have evaluated two structurally related compounds, gastrodigenin and gastrodin, for their actions on different types of ionic currents in pituitary cells and hippocampal neurons. In pituitary GH_3 lactotrophs, gastrodigenin and gastrodin suppressed the amplitude of $I_{K(M)}$ in a time- and concentration-dependent manner [137]. The IC_{50} value of gastrodigenin and gastrodin needed to inhibit $I_{K(M)}$ in GH_3 cells were estimated to be 12.1 and 19.4 ◎M, respectively [137]. Gastrodigenin-induced inhibition of $I_{K(M)}$ was associated with a slowing of the activation time course of $I_{K(M)}$, while gastrodin-mediated inhibition was associated with an increase in the activation time

 doi:10.20944/preprints202603.0263.v1

course of the current. Gastrodigenin shifted the steady-state activation curve of $I_{K(M)}$ toward less depolarized potential with no change in the gating charge of the current [137]. The addition of gastrodigenin or gastrodin also effectively inhibited $I_{K(M)}$ amplitude in hippocampal mHippoE-14 neurons. Therefore, because gastrodin can penetrate through the blood-brain barrier, different types of ionic currents, particularly low-threshold $I_{K(M)}$ with a slowly activating and deactivating properties, may be a relevant target for the regulatory actions of these agents in endocrine or neuroendocrine cells, or central neurons, if similar in vivo findings occur [134–137].

5.6. Pterostilbene

Pterostilbene (trans-3,5-dimethoxy-4′-hydroxystilbene) is a natural dimethylated analog of resveratrol isolated from *Pterocarpus marsupium* Roxb. (Fabaceae), a tree native to India, Nepal, and Sri Lanka. The extracts of *P. marsupium* containing pterostilbene have been traditionally used in Ayurvedic medicine for treating various disorders [138]. This compound has been reported to have benefits for the prevention or treatment of different kinds of cancers, as mounting evidence has demonstrated its inhibitory effects on almost every cellular event that promotes tumor progression toward metastasis in both apoptosis-dependent and apoptosis-independent manners [139–141].

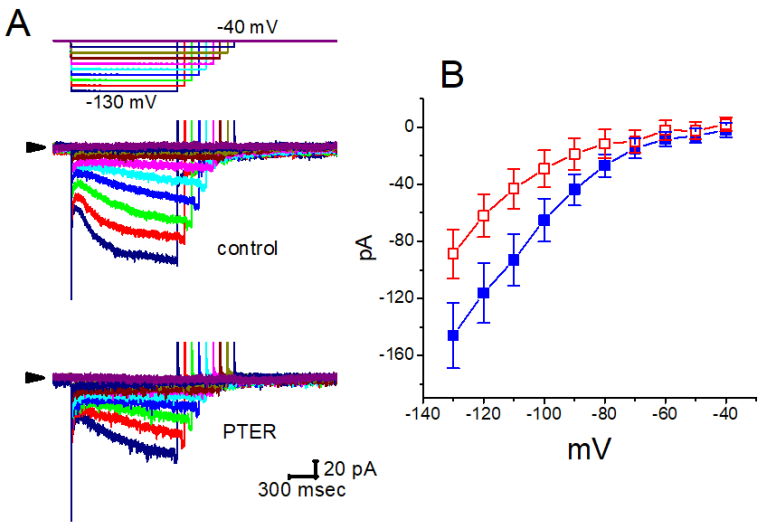

Figure 10. Effect of pterostilbene (PTER) on the current-voltage (I-V) relationships of I_h in GH$_3$ cells. Current traces were recorded during 2-sec voltage steps to a family of membrane potentials ranging between −130 and −40 mV in 10-mV steps from a holding potential of −40 mV, as indicated in the uppermost part of **(A)**. **(A)** Representative I_h traces achieved under the control condition (i.e., pterostilbene was not present) (upper) and during the exposure to 1 ◎M pterostilbene (lower). Arrowhead in each panel depicts the zero-current level and the calibration mark shown in the right lower side applies to all current traces. Of note, there are varying durations in voltage-clamp profile for better illustration. **(B)** Averaged I-V relations of I_h achieved in the absence (■) and presence (□) of 1 ◎M pterostilbene (mean ± SEM; n = 9 for each data point). Current amplitude was measured at the end of each voltage step. This figure is adapted from Ref. [142] and is published under the Creative Commons Attribution (CC BY) license.

In earlier studies, the addition of pterostilbene inhibited I_h effectively in a concentration- and time-dependent manner in pituitary GH$_3$ cells. **T**he I-V relationships of I_h established at various levels of hyperpolarizing steps were also established and depicted in **Figure 10**. It was noted that the presence of pterostilbene (1 ◎M) significantly reduced the slope of the linear fit of I_h amplitudes to the voltages between −130 and −100 mV from 27.2 ± 1.3 to 13.1 ± 1.1 nS (n = 8, $p < 0.05$). The steady state activation curve of I_h was distinctly shifted to more hyperpolarizing potentials by 11 mV, producing channel opening at more negative voltages. The results thus demonstrate that pterostilbene has a conceivable depressant action on I_h functionally expressed in GH$_3$ cells [142].

 doi:10.20944/preprints202603.0263.v1

Furthermore, as shown in **Figure 11**, the presence of pterostilbene raised the amplitude of macroscopic $I_{K(Ca)}$ in GH_3 cells. In this set of whole-cell current recordings, GH_3 cells were bathed in normal Tyrode's solution containing 1.8 mM $CaCl_2$, and the recording pipette was filled with a K^+-enriched solution. In an attempt to inactivate most of the voltage-gated K^+ currents [143], we then maintained the examined cells at the level of 0 mV, and then applied a series of voltage pulses between 0 and +50 mV with 10-mV steps. Within 1 min of exposing GH_3 cells to pterostilbene (3 ◎M), the amplitude of $I_{K(Ca)}$ elicited by this voltage profile evidently rose (**Figure 11**). For example, the addition of 3 ◎M pterostilbene increased $I_{K(Ca)}$ amplitude elicited by depolarizing pulse from 0 to +50 mV from 568 ± 35 to 1005 ± 89 pA (n = 8, $p < 0.05$). As the compound was washed out, current amplitude returned to 621 ± 38 pA (n = 8). The averaged I-V relationships of $I_{K(Ca)}$ amplitude in the control, during the exposure to 3 ◎M pterostilbene and after washout of the compound were depicted in **Figure 11B**. The addition of 3 ◎M pterostilbene substantially increased the whole-cell conductance of $I_{K(Ca)}$ measured at the voltages between +30 and +50 mV to 19.6 ± 0.8 nS (n = 8, $p < 0.05$) from control value of 12.6 ± 0.5 nS (n = 8). Therefore, pterostilbene can increase the amplitude of $I_{K(Ca)}$ observed in these cells and its stimulation of $I_{K(Ca)}$ was largely attributable to the activation of large-conductance Ca^{2+}-activated K^+ channels [142].

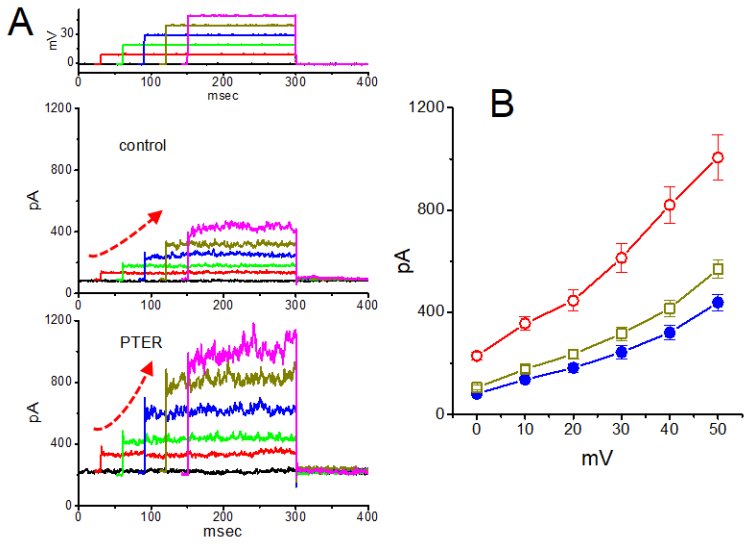

Figure 11. Stimulatory effect of pterostilbene (PTER) on Ca^{2+}-activated K^+ current ($I_{K(Ca)}$) identified in GH_3 cells. This set of whole-cell current recordings was conducted in cells suspended in normal Tyrode's solution which contained 1.8 mM $CaCl_2$. **(A)** Representative $I_{K(Ca)}$ traces obtained during the voltage steps to various membrane potentials between 0 and +50 mV in 10-mV steps from a holding potential of 0 mV (as indicated in the uppermost part of **(A)**). Records shown in the upper and lower panels were obtained under control condition and during the exposure to 3 ◎M pterostilbene, respectively. The uppermost part depicts the voltage pulses applied. The red dashed curved arrow indicates that the amplitude of $I_{K(Ca)}$ increases as the cell membrane depolarizes, demonstrating its outwardly rectifying properties. **(B)** Averaged I-V relations of $I_{K(Ca)}$ obtained in the control (●), during the exposure to 3 ◎M pterostilbene (○), and after washout of the agent (□) (mean ± SEM; n = 8 for each data point). This figure is adapted from Ref. [142] and is published under the Creative Commons Attribution (CC BY) license.

6. Other Aromatic or Conjugated Systems

6.1. Isoplumbagin and Plumbagin

Isoplumbagin (5-hydroxy-3-methyl-1,4-naphthoquinone) is a naturally occurring quinone from *Lawsonia inermis* (Lythraceae) or *Plumbago europarea* (Plumbaginaceae) [144] . Similar to isoplumbagin, plumbagin (5-hydroxy-2-methyl-1,4-naphthoquinone), another hydroxyl-1,4-napththoquinone, is another alkaloid obtained from the roots of the plants of *Plumbago* genus. Isoplumbagin and

 doi:10.20944/preprints202603.0263.v1

plumbagin have been demonstrated to exert antineoplastic activity against an array of cancer cells, including oral and tongue squamous cell carcinoma, glioblastoma, non-small cell lung carcinoma, and breast, cervical, endometrial, pancreatic and prostate cancers [145,146]. Alternatively, plumbagin was shown to induce apoptotic changes in lung cancer and neuronal cells via caspase-9 activation and targeting mitochondrial-mediated ROS induction [147,148]. Plumbagin has been reported to modify release of pituitary gonadotropin [149]. Previous studies have shown the ability of 2-mercaptophenyl-1,4-naphthoquinone, a naphthoquinone derivative, to overcome the elevation of intracellular Ca^{2+} in platelets caused by ADP and collagen [150], as well as to suppress the amplitude of $I_{K(Ca)}$ and $I_{K(DR)}$ in GH_3 cells [151].

Emerging evidence has shown that isoplumbagin modulates the magnitude, gating kinetics, and voltage-dependent hysteresis of *erg* (*ether-à-go-go*-related gene)-mediated K^+ currents ($I_{K(erg)}$) obtained in GH_3 cells [152]. In addition, these K^+ currents in MA-10 Leydig tumor cells were also found to be blocked by isoplumbagin [152]. The experimental observations suggest that the reduction by isoplumbagin or plumbagin of $I_{K(erg)}$ could potentially contribute to its anti-neoplastic actions, presuming that similar in vivo findings occur.

The IC_{50} values required for isoplumbagin-mediated block of peak or sustained $I_{K(erg)}$ were 18.3 or 2.4 ◎M, respectively [152]. From the first-order reaction scheme, the K_D value was quantitatively calculated to be 2.58 ◎M, a value that was noted to dovetail with the IC_{50} (i.e., 2.4 ◎M) for isoplumbagin-induced inhibition of sustained $I_{K(erg)}$ evoked by long-lasting membrane hyperpolarization. An earlier study has shown that the isoplumbagin at a concentration of 2.5 ◎M could suppress the activity of mitochondrial respiration through a mechanism of its inhibitory action on complex IV activation [153]. Moreover, any modifications by isoplumbagin or plumbagin of $I_{K(erg)}$ depend not only on the concentration of these compounds given but also on different confounding variables, such as the pre-existing level of the resting potential and various discharge patterns of action potentials or their combinations, presuming that the magnitude of $I_{K(erg)}$ is adequately expressed in the cells examined. Therefore, whatever the detailed mechanism of isoplumbagin-inhibited actions on $I_{K(erg)}$ remains unresolved, the block by isoplumbagin or plumbagin of $I_{K(erg)}$ would be of pharmacological relevance [154]. It is likely that the presence of isoplumbagin or plumbagin may induce prolactin secretion in vivo directly through the inhibition of $I_{K(erg)}$ [155,156]. However, to what extent isoplumbagin-mediated block of $I_{K(erg)}$ affects cardiac function [156,157] remains to be delineated.

6.2. Verteporfin

Verteporfin (Visudyne®), a benzoporphyrin derivative, is a compound therapeutically tailored as a photosensitizer for photodynamic therapy, because this agent can effectively eliminate aberrant blood vessels in the eye associated with conditions such as either the wet form of macular degeneration or abnormal choroidal neovascularization [158–160].

The photodynamic therapy with different photosensitizers such as hypericin or verteporfin has been previously demonstrated to be effective in the treatment of different types of hyperplastic or neoplastic tissues, including the residual small tumor in the pituitary gland [161,162]. Previous work indeed reported the capability of photosensitizers (e.g., rose Bengal, a fluorescein-derivative photosensitizer) to modify membrane ionic current in GH_3 cells and heart cells [163]. Alternatively, earlier reports have also revealed that verteporfin could induce anterior ischemic optic neuropathy in rodents [158,164].

A previous report discloses important findings showing that verteporfin produced a stimulatory effect on Ca^{2+}-activated K^+ current ($I_{K(Ca)}$) in pituitary GH_3 cells; however, it mildly depressed $I_{K(DR)}$ amplitude with no modification of I_{Na} or $I_{K(M)}$ [165]. The stimulatory effect on $I_{K(Ca)}$ caused by verteporfin was presumably related to changes in the level of intracellular Ca^{2+} concentrations. The results showing that removal of extracellular Ca^{2+} suppressed verteporfin-induced increase in $I_{K(Ca)}$ also suggest that extracellular Ca^{2+} and internal Ca^{2+} release both contribute to the increase in the amplitude of $I_{K(Ca)}$ in these cells.

 doi:10.20944/preprints202603.0263.v1

The EC_{50} value for either verteporfin-induced stimulation of $I_{K(Ca)}$ observed in pituitary GH_3 cells or increase in the activity of large-conductance Ca^{2+}-activated K^+ channels in 13-06-MG glioma cells (a human glioblastoma multiforme cell line) was estimated to be 2.4 or 1.9 ◎M, respectively [165]. These values are quite close to those that are either therapeutically achievable or required for the inhibitory actions on YAP-TEAD (YAP-TEA domain transcription factor) complex in different types of anaplastic or neoplastic cells [166,167]. Because verteporfin increased $I_{K(Ca)}$ amplitude within minutes in GH_3 cells, it is plausible to suggest a mechanistic association between its anti-neoplastic effects and its stimulatory actions on $I_{K(Ca)}$, possibly occurring before the compound passes through the cell membrane [1,165,168].

7. Conclusions

This review illustrates that five major chemical classes of phytoconstituents exert distinct and specific modulatory effects on membrane ionic currents, providing a mechanistic basis for their potential pharmacological activities. Alkaloids predominantly exert inhibitory effects on voltage-gated K^+ currents; however, aconitine specifically affects the inactivation of I_{Na} and $I_{K(DR)}$. Terpenoids modulate $I_{K(M)}$, I_h, and $I_{K(DR)}$. Compounds within the lignan and acetogenin groups exhibit inhibitory actions on I_{Na} and I_h. Polyphenolic compounds influence, to varying extents, $I_{K(DR)}$, I_{Na}, I_h, $I_{K(erg)}$, $I_{K(M)}$, and $I_{K(Ca)}$. In contrast, other aromatic or conjugated compounds can regulate $I_{K(erg)}$ and $I_{K(Ca)}$. Moreover, individual phytoconstituents also display distinct specificities with respect to both the amplitude and gating kinetics of different ionic currents across various cell types.

Ion channel gating kinetics refers to the dynamic rates governing transitions among the functional states of a channel—closed, open, and inactivated—and encompasses activation, inactivation, deactivation, and recovery kinetics [111,169]. By utilizing electrophysiological techniques—particularly voltage-clamp methods—and incorporating digital-to-analog conversion to generate a variety of voltage-clamp profiles, this approach remains the principal method currently used to investigate voltage-clamp ionic currents [169,170]. The docking predictions also indicate that several amino acid residues within many ion channel structures are capable of forming molecular interactions with various phytoconstituents, including hydrogen bonds and hydrophobic contacts. Collectively, these findings have important pharmacological and toxicological implications for the various bioactivities of individual phytoconstituents [1–4,171].

In addition, phytoconstituents often modulate ion channel proteins situated on the cell surface or interact with nearby membrane phospholipids. Because these actions occur at or within the plasma membrane, the compounds do not necessarily need to enter the cell. As a result, their effects typically appear rapidly and extremely low concentrations are not required for efficacy [171]. In contrast, when their targets reside within the cytoplasm—such as intracellular signaling pathways—or within the nucleus, where they influence transcriptional or epigenetic processes, the onset of action is generally slower. Access to these intracellular targets requires the compounds to cross the plasma membrane, a process largely determined by their lipid solubility (e.g., reflected by the partition coefficient). Consequently, although some bioactive phytoconstituents appear to demonstrate biological effects at relatively low concentrations in cell-free assays, such as western blotting, immunofluorescent assay, and co-immunoprecipitation [2,3,16,23,24,59,79,100,139], substantially higher concentrations are often required to elicit measurable intracellular responses [171].

It is also important to recognize that, in addition to the phytoconstituents described in this article, numerous other compounds with significant modulatory effects on ion channels are likely to be discovered as electrophysiological methodologies—such as automated patch-clamp recording—continue to advance and gain wider application. Moreover, with the exception of certain ligand-gated channels and transient receptor potential (TRP) channels, voltage-gated ion currents are typically activated either rapidly—within a few milliseconds (e.g., I_{Na})—or more slowly, over seconds (e.g., $I_{K(erg)}$ and I_h) [1,43,169,170]. Moreover, the magnitude, gating kinetics, and voltage-dependent hysteresis of voltage-gated ionic currents vary significantly across different cell types [43,152,154,169,170]. In contrast, antineoplastic or antioxidative effects generally require several

 doi:10.20944/preprints202603.0263.v1

hours to become apparent. Therefore, clarifying how rapid modulation of ion channels can ultimately translate into these slower antineoplastic, antioxidative, or immunomodulatory outcomes represents an important direction for future research [1]. Addressing this temporal gap is an important objective for future research and may uncover ion channel activity as an early initiator of subsequent intracellular (cytoplasmic or nuclear) responses [1,171].

Author Contributions: Conceptualization, S.N.W., G.F., Y.J.W., and R.L.; methodology, S.N.W. and Y.J.W.; validation, S.N.W, G.F., and Y.J.W.; formal analysis, S.N.W.; investigation, S.N.W., Y.J.W., and R.L.; resources, S.N.W. and R.L.; data curation, S.N.W., G.F., Y.J.W., and R.L.; writing—original draft preparation, S.N.W..; writing—review and editing, S.N.W. and R.L.; visualization, S.N.W. and G.F.; supervision, S.N.W.; project administration, R.L.; funding acquisition, R.L. All authors have read and agreed to the published version of the manuscript.".

Funding: This work was supported in part by the National Science and Technology Council, Taiwan (NSTC-112-2923-B-006-0016-028), and by An Nan Hospital, Taiwan (ANHRF112-43 and ANHRF112-44). This research was also funded by the Lithuania-Latvia-Taiwan collaborative project. All conclusions, recommendations, and expressed opinions within this work are based on the authors' independent research. They do not reflect the official policies or views of the funding organizations or institutions that supported this research.

Institutional Review Board Statement: Not applicable.

Data Availability Statement: The data are available upon reasonable request to the corresponding author.

Acknowledgments: The author (S.N.W.) thanks Professor Dr. Rasa Liutkevičienė for the invitation to visit the *Museum of the History of Lithuanian Medicine and Pharmacy, Kaunas, Lithuania,* which provided inspiration for this work.

Conflicts of Interest: The authors declare that they have no conflict of interest, financial or otherwise. The content and writing of this paper are entirely the responsibility of the authors.

Abbreviations

The following abbreviations are used in this manuscript:

erg	*ether-à-go-go*-related gene
HCN channel	Hyperpolarization-activated cyclic nucleotide-gated channel
IC_{50}	Concentration required for half-maximal inhibition
I_h	Hyperpolarization-activated cation current
$I_{K(Ca)}$	Ca^{2+}-activated K^+ current
$I_{K(DR)}$	Delayed-rectifier K^+ current
$I_{K(erg)}$	*erg*-mediated K^+ current
$I_{K(M)}$	M-type K^+ current
I_{Na}	Voltage-gated Na^+ current
Nav (SCN) channel	Voltage-gated Na^+ channel
I-V relationship	Current versus voltage relationship

References

1. Rao, R.; Mohammed, C.; Alschuler, L.; Pomeranz Krummel, D.A.; Sengupta, S. Phytochemical Modulation of Ion Channels in Oncologic Symptomatology and Treatment. *Cancers* (Basel) **2024**, *16*, 1786. doi: 10.3390/cancers16091786.
2. Ansari, P.; Reberio, A.D.; Ansari, N.J.; Kumar, S.; Khan, J.T.; Chowdhury, S.; Abd El-Mordy, F.M.; Hannan, J.M.A.; Flatt, P.R.; Abdel-Wahab, Y.H.A.; Seidel, V. Therapeutic Potential of Medicinal Plants and Their Phytoconstituents in Diabetes, Cancer, Infections, Cardiovascular Diseases, Inflammation and Gastrointestinal Disorders. *Biomedicines* **2025**, *13*, 454. doi: 10.3390/biomedicines13020454.
3. Sonnino, R.; Ciccarelli, G.; Moffa, S.; Soldovieri, L.; Di Giuseppe, G.; Brunetti, M.; Cinti, F.; Di Piazza, E.; Gasbarrini, A.; Nista, E.C.; Pontecorvi, A.; Giaccari, A.; Mezza, T. Exploring nutraceutical approaches

 doi:10.20944/preprints202603.0263.v1

linking metabolic syndrome and cognitive impairment. *iScience* **2025**, *28*, 111848. doi: 10.1016/j.isci.2025.111848.

4. Froldi, G. Bioactivity of Natural Compounds: From Plants to Humans. *Molecules* **2026**, *31*, 295. doi: 10.3390/molecules31020295.
5. Pullela, R.; Young, L.; Gallagher, B.; Avis, S.P.; Randell, E.W. A case of fatal aconitine poisoning by Monkshood ingestion. *J. Forensic Sci.* **2008**, *53*, 491-494. doi: 10.1111/j.1556-4029.2007.00647.x.
6. Gao, Y.; Fan, H.; Nie, A.; Yang, K.; Xing, H.; Gao, Z.; Yang, L.; Wang, Z.; Zhang, L. Aconitine: A review of its pharmacokinetics, pharmacology, toxicology and detoxification. *J. Ethnopharmacol.* **2022**, *293*, 115270. doi: 10.1016/j.jep.2022.115270.
7. Wang, S.Y.; Wang, G.K. Voltage-gated sodium channels as primary targets of diverse lipid-soluble neurotoxins. *Cell. Signal.* **2003**, *15*, 151-159. doi: 10.1016/s0898-6568(02)00085-2.
8. Zhang, Y.; Wang, Y.P.; Guo, S.; Li, T.T.; Wang, Q.Y.; Zhang, X.; Zheng, Y.M.; Wen, Y.Q.; Meng, F.H.; Zhang, T.J. Novel E-F ring derivatives of aconitine scaffold as potent Hsp90 inhibitors for the treatment of colorectal cancer. *Eur. J. Med. Chem.* **2025**, *296*, 117895. doi: 10.1016/j.ejmech.2025.117895.
9. Lin, M.W.; Wang, Y.J.; Liu, S.I.; Lin, A.A.; Lo, Y.C.; Wu, S.N. Characterization of aconitine-induced block of delayed rectifier K^+ current in differentiated NG108-15 neuronal cells. *Neuropharmacology* **2008**, *54*, 912-923. doi: 10.1016/j.neuropharm.2008.01.009.
10. Wang, Y.J.; Chen, B.S.; Lin, M.W.; Lin, A.A.; Peng, H.; Sung, R.J.; Wu, S.N. Time-dependent block of ultrarapid-delayed rectifier K^+ currents by aconitine, a potent cardiotoxin, in heart-derived H9c2 myoblasts and in neonatal rat ventricular myocytes. *Toxicol. Sci.* **2008**, *106*, 454-463. doi: 10.1093/toxsci/kfn189.
11. Wu, S.N.; Chen, B.S.; Lin, M.W.; Liu, Y.C. Contribution of slowly inactivating potassium current to delayed firing of action potentials in NG108-15 neuronal cells: experimental and theoretical studies. *J. Theor. Biol.* **2008**, *252*, 711-721. doi: 10.1016/j.jtbi.2008.01.031.
12. Wu, S.N.; Chen, B.S.; Lo, Y.C. Evidence for aconitine-induced inhibition of delayed rectifier K^+ current in Jurkat T-lymphocytes. *Toxicology* **2011**, *289*, 11-18. doi: 10.1016/j.tox.2011.07.003.
13. Chou, C.J.; So, E.C. Effects of aconitine on membrane currents and action potentials in neonatal rat ventricular myocytes and its impact on electrocardiographic changes. *Medical Research Archives* **2024**, *12*, ISSN 2375-1924. doi: https://doi.org/10.18103/mra.v12i3.5190.
14. Lee, C.H.; Chiang, S.L.; Ko, A.M.; Hua, C.H.; Tsai, M.H.; Warnakulasuriya, S.; Ibrahim, S.O.; Sunarjo, Zain, R.B.; Ling, T.Y.; Huang, C.L.; Lane, H.Y.; Lin, C.C.; Ko, Y.C. Betel-quid dependence domains and syndrome associated with betel-quid ingredients among chewers: an Asian multi-country evidence. *Addiction* **2014**, *109*, 1194-1204. doi: 10.1111/add.12530.
15. Li, M.; Gao, F.; Zhou, Z.S.; Zhang, H.M.; Zhang, R.; Wu, Y.F.; Bai, M.H.; Li, J.J.; Lin, S.R.; Peng, JY. Arecoline inhibits epithelial cell viability by upregulating the apoptosis pathway: implication for oral submucous fibrosis. *Oncol Rep.* **2014**, *31*, 2422-2428. doi: 10.3892/or.2014.3091.
16. Chan, P.K.; Keyes, A.; Papanastasiou, S.; Sarrafpour, B.; Ramaswamy, Y.; Co, S.; Zoellner, H.; Chami, B. Arecoline stimulates the IL-33/13 axis and upregulates pro-fibrotic CTGF: A possible role in oral submucous fibrosis. *Food Chem. Toxicol.* **2026**, *207*, 115811. doi: 10.1016/j.fct.2025.115811.
17. Lee, S.C.; Tsai, C.C.; Yao, C.H.; Hsu, Y.M.; Chen, Y.S.; Wu, M.C. Effect of arecoline on regeneration of injured peripheral nerves. *Am. J. Chin. Med.* **2013**, *41*, 865-885. doi: 10.1142/S0192415X13500584.
18. So, E.C.; Huang, Y.M.; Hsing, C.H.; Liao, Y.K.; Wu, S.N. Arecoline inhibits intermediate-conductance calcium-activated potassium channels in human glioblastoma cell lines. *Eur. J. Pharmacol.* **2015**, *758*, 177-187. doi: 10.1016/j.ejphar.2015.03.065.
19. Xu, H.; Lai, W.; Zhang, Y.; Liu, L.; Luo, X.; Zeng, Y.; Wu, H.; Lan, Q.; Chu, Z. Tumor-associated macrophage-derived IL-6 and IL-8 enhance invasive activity of LoVo cells induced by PRL-3 in a KCNN4 channel-dependent manner. *BMC Cancer* **2014**, *14*, 330. doi: 10.1186/1471-2407-14-330.
20. Bova, S.; Padrini, R.; Goldman, W.F.; Berman, D.M.; Cargnelli, G. On the mechanism of vasodilating action of berberine: possible role of inositol lipid signaling system. *J. Pharmacol. Exp. Ther.* **1992**, *261*, 318-323.
21. Chi, C.W.; Chang, Y.F.; Chao, T.W.; Chiang, S.H.; P'eng, F.K.; Lui, W.Y.; Liu, T.Y. Flowcytometric analysis of the effect of berberine on the expression of glucocorticoid receptors in human hepatoma HepG2 cells. *Life Sci.* **1994**, *54*, 2099-2107. doi: 10.1016/0024-3205(94)00719-5.

 doi:10.20944/preprints202603.0263.v1

22. Wu, S.N.; Yu, H.S.; Jan, C.R.; Li, H.F.; Yu, C.L. Inhibitory effects of berberine on voltage- and calcium-activated potassium currents in human myeloma cells. *Life Sci.* **1998**, *62*, 2283-2294. doi: 10.1016/s0024-3205(98)00209-4.
23. Hsu, Y.Y.; Chen, C.S.; Wu, S.N.; Jong, Y.J.; Lo, Y.C. Berberine activates Nrf2 nuclear translocation and protects against oxidative damage via a phosphatidylinositol 3-kinase/Akt-dependent mechanism in NSC34 motor neuron-like cells. *Eur. J. Pharm. Sci.* **2012**, *46*, 415-425. doi: 10.1016/j.ejps.2012.03.004.
24. Bian, X.; Guo, Q.; Yau, L.F.; Yang, L.; Wang, X.; Zhao, S.; Wu, S.; Qin, X.; Jiang, Z.H.; Li, C. Berberine-inspired ionizable lipid for self-structure stabilization and brain targeting delivery of nucleic acid therapeutics. *Nat. Commun.* **2025**, *16*, 2368. doi: 10.1038/s41467-025-57488-0.
25. Zhou, W.; Asif, A.; Situ, C.; Wang, J.; Hao, H. Multiple target and regulatory pathways of berberine. *Phytomedicine* **2025**, *146*, 157030. doi: 10.1016/j.phymed.2025.157030.
26. Moskalev, A.; Veselova, O. Potential dietary geroprotectors and their impact on key mechanisms of aging. *Biogerontology* **2026**, *27*, 8. https://doi.org/10.1007/s10522-025-10355-3.
27. Britch, S.C.; Babalonis, S.; Walsh, S.L. Cannabidiol: pharmacology and therapeutic targets. *Psychopharmacology* (Berl) **2021**, *238*, 9-28. doi: 10.1007/s00213-020-05712-8.
28. Huang, C.W.; Lin, P.C.; Chen, J.L.; Lee, M.J. Cannabidiol Selectively Binds to the Voltage-Gated Sodium Channel Na(v)1.4 in Its Slow-Inactivated State and Inhibits Sodium Current. *Biomedicines* **2021**, *9*, 1141.
29. Ghovanloo, M.R.; Ruben, P.C. Cannabidiol and Sodium Channel Pharmacology: General Overview, Mechanism, and Clinical Implications. *Neuroscientist* **2022**, *28*, 318–334.
30. Liu, Y.C.; So, E.C.; Wu, S.N. Cannabidiol Modulates M-Type K^+ and Hyperpolarization-Activated Cation Currents. *Biomedicines* **2023**, *11*, 2651. doi: 10.3390/biomedicines11102651.
31. Giang, P.M.; Son, P.T.; Lee, J.J.; Otsuka, H. Four *ent*-kaurane-type diterpenoids from *Croton tonkinensis* GAGNEP. *Chem. Pharm. Bull.* (Tokyo) **2004**, *52*, 879-882. doi: 10.1248/cpb.52.879.
32. Lee, H.M.; Kuo, P.C.; Chen, W.H.; Chen, P.J.; Lam, S.H.; Su, Y.C.; Chen, C.H. Diterpenoid from *Croton tonkinensis* as a Potential Radiation Sensitizer in Oral Squamous Cell Carcinoma: An In Vitro Study. *Int. J. Mol. Sci.* **2024**, *25*, 11839. doi: 10.3390/ijms252111839.
33. Hsiao, H.T.; Lee, Y.C.; Liu, Y.C.; Kuo, P.C.; Wu, S,N. Differential suppression of delayed-rectifier and inwardly rectifier K^+ currents by a group of *ent*-kaurane-type diterpenoids from *Croton tonkinensis*, in microglial cells. *Eur. J. Pharmacol.* **2019**, *856*, 172414. doi: 10.1016/j.ejphar.2019.172414.
34. Kuo, P.C.; Liu, Y.C.; Lo, Y.C.; Wu, S.N. Characterization of Inhibitory Effectiveness in Hyperpolarization-Activated Cation Currents by a Group of *ent*-Kaurane-Type Diterpenoids from *Croton tonkinensis*. *Int. J. Mol. Sci.* **2020**, *21*, 1268. doi: 10.3390/ijms21041268.
35. Mitra, S.; Rauf, A.; Tareq, A.M.; Jahan, S.; Emran, T.B.; Shahriar, T.G.; Dhama, K.; Alhumaydhi, F.A.; Aljohani, A.S.M.; Rebezov, M.; Uddin, M.S.; Jeandet, P.; Shah, Z.A.; Shariati, M.A.; Rengasamy, K.R. Potential health benefits of carotenoid lutein: An updated review. *Food Chem. Toxicol.* **2021**, *154*, 112328. doi: 10.1016/j.fct.2021.112328.
36. Mrowicka, M.; Mrowicki, J.; Kucharska, E.; Majsterek, I. Lutein and Zeaxanthin and Their Roles in Age-Related Macular Degeneration-Neurodegenerative Disease. *Nutrients* **2022**, *14*, 827. doi: 10.3390/nu14040827.
37. Chuang, C.W.; Chang, K.P.; Cho, H.Y.; Chuang, T.H.; Yu, M.C.; Wu, C.L.; Wu, S.N. Characterization of Inhibitory Capability on Hyperpolarization-Activated Cation Current Caused by Lutein (β,ε-Carotene-3,3'-Diol), a Dietary Xanthophyll Carotenoid. *Int. J. Mol. Sci.* **2022**, *23*, 7186. doi: 10.3390/ijms23137186.
38. Dini, L.; Del Lungo, M.; Resta, F.; Melchiorre, M.; Spinelli, V.; Di Cesare Mannelli, L.; Ghelardini, C.; Laurino, A.; Sartiani, L.; Coppini, R.; Mannaioni, G.; Cerbai, E.; Romanelli, M.N. Selective Blockade of HCN1/HCN2 Channels as a Potential Pharmacological Strategy Against Pain. *Front. Pharmacol.* **2018**, *9*, 1252. doi: 10.3389/fphar.2018.01252.
39. Hsiao, H.T.; Liu, Y.C.; Liu, P.Y.; Wu, S.N. Concerted suppression of I_h and activation of $I_{K(M)}$ by ivabradine, an HCN-channel inhibitor, in pituitary cells and hippocampal neurons. *Brain Res. Bull.* **2019**, *149*, 11-20. doi: 10.1016/j.brainresbull.2019.03.016.

 doi:10.20944/preprints202603.0263.v1

40. Wu, S.N.; Fang, Y.H.; Liu, P.Y.; Liu, Y.W. Characterization of hyperpolarization-induced cation current in differentiated human embryonic stem cell-derived cardiomyocytes. *Journal of the American College of Cardiology* (JACC) **2020**, *75* (Suppl), P31322-X.
41. Nache, V.; Eick, T.; Schulz, E.; Schmauder, R.; Benndorf, K. Hysteresis of ligand binding in CNGA2 ion channels. *Nat. Commun.* **2013**, *4*, 2866. doi: 10.1038/ncomms3866.
42. Barthel, L.; Reetz, O.; Strauss, U. Use Dependent Attenuation of Rat HCN1-Mediated Ih in Intact HEK293 Cells. *Cell. Physiol. Biochem.* **2016**, *38*, 2079–2093.
43. Xiao, Y.F.; Chandler, N.; Dobrzynski, H.; Richardson, E.S.; Tenbroek, E.M.; Wilhelm, J.J.; Sharma, V.; Varghese, A.; Boyett, M.R.; Iaizzo, P.A.; Sigg, D.C. Hysteresis in human HCN4 channels: a crucial feature potentially affecting sinoatrial node pacemaking. *Sheng Li Xue Bao* **2010**, *62*, 1-13.
44. Datunashvili, M.; Chaudhary, R.; Zobeiri, M.; Lüttjohann, A.; Mergia, E.; Baumann, A.; Balfanz, S.; Budde, B.; van Luijtelaar, G.; Pape, H.C.; Koesling, D.; Budde, T. Modulation of Hyperpolarization-Activated Inward Current and Thalamic Activity Modes by Different Cyclic Nucleotides. *Front. Cell. Neurosci.* **2018**, *12*, 369. doi: 10.3389/fncel.2018.00369.
45. Chang, W.T.; Ragazzi, E.; Liu, P.Y.; Wu, S.N. Effective block by pirfenidone, an antifibrotic pyridone compound (5-methyl-1-phenylpyridin-2[H-1]-one), on hyperpolarization-activated cation current: An additional but distinctive target. *Eur. J. Pharmacol.* **2020**, *882*, 173237. doi: 10.1016/j.ejphar.2020.173237.
46. Kodirov, S.A. Delineation and functions of HCN channels in neurons. *Prog. Biophys. Mol. Biol.* 2025, *198*, 21-31. doi: 10.1016/j.pbiomolbio.2025.09.002.
47. D'Aloisio, R.; Di Antonio, L.; Toto, L.; Rispoli, M.; Di Iorio, A.; Delvecchio, G.; Mastropasqua, R. Choroidal Changes in Blood Flow in Patients with Intermediate AMD after Oral Dietary Supplement Based on Astaxanthin, Bromelain, Vitamin D3, Folic Acid, Lutein, and Antioxidants. *Medicina* (Kaunas) **2022**, *58*, 1092. doi: 10.3390/medicina58081092.
48. Ogaard, B.; Larsson, E.; Glans, R.; Henriksson, T.; Birkhed, D. Antimicrobial effect of a chlorhexidine-thymol varnish (Cervitec) in orthodontic patients. A prospective, randomized clinical trial. *J. Orofac. Orthop.* **1997**, *58*, 206–213.
49. Kasparaviciene, G.; Kalveniene, Z.; Pavilonis, A.; Marksiene, R.; Dauksiene, J.; Bernatoniene, J. Formulation and Characterization of Potential Antifungal Oleogel with Essential Oil of Thyme. *Evid. Based Complement. Alternat. Med.* **2018**, *2018*, 9431819. doi: 10.1155/2018/9431819.
50. Aksoy, T.; Kilimcioğlu, A.A. Thymol's antileishmanial activity and its impact on host cytokine profiles: In vitro and ex vivo studies on Leishmania tropica. *Parasitol. Int.* **2026**, *110*, 103139. doi: 10.1016/j.parint.2025.103139.
51. Chen, C.; Liu, L.; Tang, S.; Li, D.; Dai, C. Antifungal Activity of Natural Thymol: Advances on Molecular Mechanisms and Therapeutic Potential. *Biomolecules* **2026**, *16*, 149. doi: 10.3390/biom16010149.
52. Hoo, G.W.; Hinds, R.L.; Dinovo, E.; Renner, S.W. Fatal large-volume mouthwash ingestion in an adult: a review and the possible role of phenolic compound toxicity. *J. Intensive Care Med.* **2003**, *18*, 150-155.
53. Dee Manuel, M.P.; Shih, Y.H.; Hsia, S.M.; Wang, T.H.; Tseng, Y.H.; Tu, M.G.; Shieh, T.M. Evaluating thymol vapor for biofilm removal and biocompatibility in curved root canal models in vitro. *J. Dent. Sci.* **2026**, *21*, 323-332. doi: 10.1016/j.jds.2025.09.001.
54. Shen, A.Y.; Huang, M.H.; Wang, T.S.; Wu, H.M.; Kang, Y.F, Chen CL. Thymol-evoked Ca^{2+} mobilization and ion currents in pituitary GH_3 cells. *Nat. Prod. Commun.* **2009**, *4*, 749-752.
55. Huang, M.H.; Wu, S.N.; Shen, A.Y. Stimulatory actions of thymol, a natural product, on Ca^{2+}-activated K^+ current in pituitary GH_3 cells. *Planta Med.* **2005**, *71*, 1093-1098. doi: 10.1055/s-2005-873124.
56. Zheng, Y.; Zhang, W.J.; Wang, X.M. Triptolide with potential medicinal value for diseases of the central nervous system. *CNS Neurosci. Ther.* **2013**, *19*, 76-82.
57. Chen, L.W.; Wang, Y.Q.; Wei, L.C.; Shi, M.; Chan, Y.S. Chinese herbs and herbal extracts for neuroprotection of dopaminergic neurons and potential therapeutic treatment of Parkinson's disease. *CNS Neurol. Disord. Drug Targets* **2007**, *6*, 273-281.
58. Su, Z.; Yuan, Y.; Cao, L.; Zhu, Y.; Gao, L.; Qiu, Y.; He, C. Triptolide promotes spinal cord repair by inhibiting astrogliosis and inflammation. *Glia* **2010**, *58*, 901-915.

 doi:10.20944/preprints202603.0263.v1

59. Zhang, H.; Zhu, W.; Su, X.; Wu, S.; Lin, Y.; Li, J.; Wang, Y.; Chen, J.; Zhou, Y.; Qiu, P.; Yan, G.; Zhao, S.; Hu, J.; Zhang, J. Triptolide inhibits proliferation and invasion of malignant glioma cells. *J. Neurooncol.* **2012**, *109*, 53-62.
60. Lin, J.; Chen, L.Y.; Lin, Z.X.; Zhao, M.L. The effect of triptolide on apoptosis of glioblastoma multiforme (GLM) cells. *J. Int. Med. Res.* **2007**, *35*, 637-643.
61. So, E.C.; Lo, Y.C.; Chen, L.T.; Kao, C.A.; Wu, S.N. High effectiveness of triptolide, an active diterpenoid triepoxide, in suppressing Kir-channel currents from human glioma cells. *Eur. J. Pharmacol.* **2014**, *738*, 332-341. doi: 10.1016/j.ejphar.2014.05.059.
62. Haj-Yasein, N.N.; Jensen, V.; Vindedal, G.F.; Gundersen, G.A.; Klungland, A.; Ottersen, O.P.; Hvalby, O.; Nagelhus, E,A. Evidence that compromised K^+ spatial buffering contributes to the epileptogenic effect of mutations in the human Kir4.1 gene (*KCNJ10*). *Glia* **2011**, *59*, 1635-1642.
63. Zhou, X.; Zhao, C.; Xu, H.; Xu, Y.; Zhan, L.; Wang, P.; He, J.; Lu, T.; Gu, Y.; Yang, Y.; Xu, C.; Chen, Y.; Liu, Y.; Zeng, Y.; Tian, F.; Chen, Q.; Xie, X.; Liu, J.; Hu, H.; Li, J.; Zheng, Y.; Guo, J.; Gao, Z. Pharmacological inhibition of Kir4.1 evokes rapid-onset antidepressant responses. *Nat. Chem. Biol.* **2024**, *20*, 857-866. doi: 10.1038/s41589-024-01555-y.
64. Wang, J.; Jiang, B.; Shan, Y.; Wang, X.; Lv, X, Mohamed J, Li H, Wang C, Chen J, Sun J. Metabolic mapping of *Schisandra chinensis* lignans and their metabolites in rats using a metaboliomic approach based on HPLC with quadrupole time-of-flight MS/MS spectrometry. *J. Sep. Sci.* **2020**, *43*, 378-388.
65. Takanche, J.S.; Kim, J.E.; Han, S.H.; Yi, H.K. Effect of gomisin A on osteoblast differentiation in high glucose-mediated oxidative stress. *Phytomedicine* 2020, *66*, 153107.
66. Hwang, I.S.; Kim, J.E.; Lee, Y.J.; Kwak, M.H.; Choi, Y.H.; Kang, B.C.; Hong, J.T.; Hwang, D.Y. Protective effects of gomisin A isolated from *Schisandra chinensis* against CCl_4-induced hepatic and renal injury. *Int. J. Mol. Med.* 2013, *31*, 888-898.
67. Kim, E.J.; Jang, M.; Lee, M.J.; Choi, J.H.; Lee, S.J.; Kim, S.K.; Jang, D.S.; Cho, I.H. *Schisandra chinensis* stem ameliorates 3-nitropropionic acid-induced striatal toxicity via activation of the Nrf2 pathway and inhibition of the MAPKs and NF-◎B pathways. *Front. Pharmacol.* 2017, *8*, 673.
68. Nam, S.Y.; Kim, K.Y.; Kim, M.H.; Jang, J.B.; Rah, S.Y.; Chae, H.J.; Lee, J.M.; Kim, H.M.; Jeong, H.J. Anti-inflammatory effects of a traditional Korean medicine: Ojayeonjonghwan. *Pharm. Bio.* 2017, *55*, 1856-1862.
69. Ye, B.H.; Lee, S.J.; Choi, Y.W.; Park, S.Y.; Kim, C.D. Preventive effect of gomisin J from Schisandra chinensis on angiotensin II-induced hypertension via an increased nitric oxide bioavailability. *Hypertens. Res.* **2015**, *38*, 169-177. doi: 10.1038/hr.2014.162.
70. Hwang, D.; Shin, S.Y.; Lee, Y.; Hyun, J.; Yong, Y.; Park, J.C.; Lee, Y.H.; Lim, Y. A compound isolated from *Schisandra chinensis* induces apoptosis. *Bioorg. Med. Chem. Lett.* 2011, 21, 6054-6057.
71. Hong, S.H.; Li, M.; Jeung, E.B.; Lee, G.S.; Hong, E.J.; Choi, Y.W.; An, B.S. Therapeutic effects of Schisandra chinensis on the hyperprolactinemia in rat. *Int. J. Oncol.* 2017, *50*, 1448-1454.
72. Chang, W.T.; Wu, S.N. Inhibitory Effectiveness of Gomisin A, a Dibenzocyclooctadiene Lignan Isolated from *Schizandra chinensis*, on the Amplitude and Gating of Voltage-Gated Na^+ Current. *Int. J. Mol. Sci.* **2020**, *21*, 8816. doi: 10.3390/ijms21228816.
73. Fujita, M.; Itokawa, H.; Sashida, Y. Studies on the components of *Magnolia obovate* Thunb. 3. Occurrence of magnolol and hõnokiol in *M. obovate* and other allied plants. *Yakugaku Zasshi* **1973**, *93*, 429-434.
74. Ong, C.P.; Lee, W.L.; Tang, Y.Q.; Yap, W.H. Honokiol: a review of its anticancer potential and mechanisms. *Cancers* (Basel) **2019**, *12*, 48.
75. Lu, C.H.; Chen, S.H.; Chang, Y.S.; Liu, Y.W.; Wu, J.Y.; Lim, Y.P.; Yu, H.I.; See, Y.R. Honokiol, a potential therapeutic agent, induces cell cycle arrest and program cell death in vitro and in vivo in human thyroid cancer cells. *Pharmacol. Res.* **2017**, *115*, 288-298.
76. Tachikawa, E.; Takahashi, M.; Kashimoto, T. Effects of extract and ingredients isolated from *Magnolia obovata* Thunberg on catecholamine secretion from bovine adrenal chromaffin cells. *Biochem. Pharmacol.* **2000**, *60*, 433-440.
77. Wang, C.; Gan, D.; Wu, J.; Liao, M.; Liao, X.; Ai, W. Honokiol exerts antidepressant effects in rats exposed to chronic unpredictable mild stress by regulating brain derived neurotrophic factor level and hypothalamus-pituitary-adrenal axis activity. *Neurochem. Res.* **2018**, *43*, 1519-1528.

 doi:10.20944/preprints202603.0263.v1

78. Chan, M.H.; Chen, H.H.; Lo, Y.C.; Wu, S.N. Effectiveness in the Block by Honokiol, a Dimerized Allylphenol from *Magnolia Officinalis*, of Hyperpolarization-Activated Cation Current and Delayed-Rectifier K^+ Current. *Int. J. Mol. Sci.* **2020**, *21*, 4260. doi: 10.3390/ijms21124260.

79. Khodir, S.A.; Sweed, E.M.; El-Haroun, H.; Abd-Elhamid, T.H.; El Derbaly, S.A.; Mahmoud, A.R.; Motawea, S.M. Honokiol ameliorates reserpine-induced fibromyalgia through antioxidant, anti-inflammatory, neurotrophic, and anti-apoptotic mechanisms. *Sci. Rep.* **2025**, *15*, 25983. doi: 10.1038/s41598-025-07209-w.

80. Shiao, M.S. Natural products of the medicinal fungus *Ganoderma lucidum*: occurrence, biological activities, and pharmacological functions. *Chem. Rec.* **2003**, *3*, 172-180.

81. Cör, D.; Knez, Ž.; Knez Hrnčič, M. Antitumour, antimicrobial, antioxidant and antiacetylcholinesterase effect of *Ganoderma lucidum* terpenoids and polysaccharides: a review. *Molecules* **2018**, *23*, 649.

82. Peng, X.; Li, L.; Dong, J.; Lu, S.; Lu, J.; Li, X.; Zhou, L.; Qiu, M. Lanostane-type triterpenoids from the fruiting bodies of *Ganoderma applanatum*. *Phytochemistry* **2019**, *157*, 103-110.

83. Kuok, Q.Y.; Yeh, C.Y.; Su, B.C.; Hsu, P.L.; Ni, H.; Liu, M.Y.; Mo, F.E. The triterpenoids of *Ganoderma tsugae* prevent stress-induced myocardial injury in mice. Mol. *Nutr. Food Res.* **2013**, *57*, 1892-1896.

84. Ma, B.; Ren, W.; Zhou, Y.; Ma, J.; Ruan, Y.; Wen, C.N. Triterpenoids form the spores of *Ganoderma lucidum*. *N. Am. J. Med. Sci.* **2011**, *3*, 495-498.

85. Lou, H.W.; Guo, X.Y.; Zhang, X.C.; Guo, L.Q.; Lin, J.F. Optimization of cultivation conditions of lingzhi or reishi medicinal mushroom, *Ganoderma lucidum* (Agaricomycetes) for the highest antioxidant activity and antioxidant content. *Int. J. Med. Mushrooms* **2019**, *21*, 353-366.

86. Liang, C.; Tian, D.; Liu, Y.; Li, H.; Zhu, J.; Li, M.; Xin, M.; Xia, J. Review of the molecular mechanisms of *Ganoderma lucidum* triterpenoids: ganoderic acids A, C2, D, F, DM, X and Y. *Eur. J. Med. Chem.* **2019**, *174*, 130-141.

87. Chang, W.T.; Gao, Z.H.; Lo, Y.C.; Wu, S.N. Evidence for Effective Inhibitory Actions on Hyperpolarization-Activated Cation Current Caused by *Ganoderma* Triterpenoids, the Main Active Constituents of *Ganoderma* Spores. *Molecules* **2019**, *24*, 4256. doi: 10.3390/molecules24234256.

88. Kim, A.Y.; Yun, C.I.; Lee, J.G.; Kim, Y.J. Determination and daily intake estimation of lignans in sesame seeds and sesame oil products in Korea. *Foods* **2020**, 9, 394.

89. Dhar, P.; Chattopadhya, K.; Bhattacharyya, D.; Biswas, A.; Roy, B.; Ghosh, S. Ameliorative influence of sesame lignans on lipid profile and lipid peroxidation in induced diabetic rats. *J. Agric. Food Chem.* **2007**, *55*, 5875-5880.

90. Liang, Y.T.; Chen, J.; Jiao, R.; Peng, C.; Zuo, Y.; Lei, L.; Liu, Y.; Wang, X.; Ma, K.Y.; Huang, Y.; Chen, Z.Y. Cholesterol-lowering activity of sesamin is associated with down-regulation on genes of sterol transporters involved in cholesterol absorption. *J. Agri. Food Chem.* **2015**, *63*, 2963-2969.

91. Ruankham, W.; Suwanjang, W.; Wongchitrat, P.; Prachayasittikul, V.; Prachayasittikul, S.; Phopin, K. Sesamin and sesamol attenuate H_2O_2-induced oxidative stress on human neuronal cells via the SIRT1-SIRT3-FOXO3a signaling pathway. *Nutr. Neurosci.* **2021**, *24*, 90-101 doi: 10.1080/1028415X.2019.1596613.

92. Jayaraj, P.; Narasimhulu, C.A.; Rajagopalan, S.; Parthasarathy, S.; Desikan, R. Sesamol: a powerful functional food ingredient from sesame oil for cardioprotection. *Food Funct.* **2020**, *11*, 1198-1210.

93. Kuo, P.C.; Kao, Z.H.; Lee, S.W.; Wu, S.N. Effects of Sesamin, the Major Furofuran Lignan of Sesame Oil, on the Amplitude and Gating of Voltage-Gated Na^+ and K^+ Currents. *Molecules* 2020, *25*, 3062. doi: 10.3390/molecules25133062.

94. Pan, Y.; Cummins, T.R. Distinct functional alterations in *SCN8A* epilepsy mutant channels. *J. Physiol.* **2020**, *598*, 381-401.

95. Djamgoz, M.B.A. Stemness of Cancer: A Study of Triple-negative Breast Cancer From a Neuroscience Perspective. *Stem Cell Rev. Rep.* **2025**, *21*, 337-350. doi: 10.1007/s12015-024-10809-0.

96. Guadano, A.; Gutierrez, C.; de La Pena, E.; Cortes, D.; Gonzalez-Coloma, A. Insecticidal and mutagenic evaluation of two *annonaceous* acetogenins. *J. Nat. Prod.* **2000**, *63*, 773-776.

97. Queiroz, E.F.; Roblot, F.; Duret, P.; Figadere, B.; Gouyette, A.; Laprevote, O.; Serani, L.; Hocquemiller, R. Synthesis, spectroscopy, and cytotoxicity of glycosylated acetogenin derivatives as promising molecules for cancer therapy. *J. Med. Chem.* **2000**, *43*, 1604-1610.

 doi:10.20944/preprints202603.0263.v1

98. Arndt, S.; Emde, U.; Baurle, S.; Friedrich, T.; Grubert, L.; Koert, U. Quinone-annonaceous acetogenins: synthesis and complex I inhibition studies of a new class of natural product hybrids. *Chemistry* **2001**, *7*, 993-1005.
99. Shimda, H.; Grutzner, J.B.; Kozlowski, J.F.; McLaughlin, J.L. Membrane conformations and their relation to cytotoxicity of asimicin and its analogues. *Biochemistry* **1998**, *37*, 854-866.
100. Zhu, X.F.; Liu, Z.C.; Xie, B.F.; Li, Z.M.; Feng, G.K.; Xie, H.H.; Wu, S.J.; Yang, R.Z.; Wei, X.Y.; Zeng, Y.X. Involvement of caspase-3 activation in squamocin-induced apoptosis in leukemia cell line HL-60. *Life Sci.* **2002**, *70*, 1259-1269.
101. Wu, S.N.; Chiang, H.T.; Chang, F.R.; Liaw, C.C.; Wu, Y.C. Stimulatory effects of squamocin, an *Annonaceous* acetogenin, on Ca^{2+}-activated K^+ current in cultured smooth muscle cells of human coronary artery. *Chem. Res. Toxicol.* **2003**, *16*, 15-22. doi: 10.1021/tx020067v.
102. Priyadarsini, K.I. The chemistry of curcumin: from extraction to therapeutic agent. *Molecules* **2014**, *19*, 20091-20112.
103. Meng, B.; Li, J.; Cao, H. Antioxidant and antiiflammatory activities of curcumin on diabetes mellitus and its complication. *Curr. Pharm. Des.* **2013**, *19*, 2101-2113.
104. Jiménez-Osorio, A.S.; Monroy, A.; Alavez, S. Curcumin and insulin resistance-Molecular targets and clinical evidences. *Biofactors* **2016**, *42*, 561-580. doi: 10.1002/biof.1302.
105. Kuo, P.C.; Yang, C.J.; Lee, Y.C.; Chen, P.C.; Liu, Y.C.; Wu, S.N. The comprehensive electrophysiological study of curcuminoids on delayed-rectifier K^+ currents in insulin-secreting cells. *Eur. J. Pharmacol.* **2018**, *819*, 233-241. doi: 10.1016/j.ejphar.2017.12.004.
106. Gutierres, V.O.; Campos, M.L.; Arcaro, C.A.; Assis, R.P.; Baldan-Cimatti, H.M.; Peccinini, R.G.; Paula-Gomes, S.; Kettelhut, I.C.; Baviera, A.M.; Brunetti, I.L: Curcumin pharmacokinetic and pharmacodynamics evidences in streptozotocin-diabetic rats support the antidiabetic activity to be via metabolite(s). *Evid. Based. Complement. Alternat. Med.* **2015**, *2015*, 678218.
107. Lim, H.J.; Lee, J.H.; Choi, J.S.; Lee, S.K.; Kim, Y.S.; Kim, H.P. Inhibition of airway inflammation by the roots of *Angelica decursiva* and its constituent, columbianadin. *J. Ethnopharmacol.* **2014**, *155*, 1353-1361. doi: 10.1016/j.jep.2014.07.033.
108. Yu, J.; Zhong, B.; Xiao, Q.; Du, L.; Hou, Y.; Sun, H.S.; Lu, J.J.; Chen, X. Induction of programmed necrosis: A novel anti-cancer strategy for natural compounds. *Pharmacol. Ther.* **2020**, *214*, 107593. doi: 10.1016/j.pharmthera.2020.107593.
109. Chang, W.T.; Wu, S.N. Effectiveness of Columbianadin, a Bioactive Coumarin Derivative, in Perturbing Transient and Persistent I_{Na}. *Int. J. Mol. Sci.* **2021**, *22*, 621. doi: 10.3390/ijms22020621.
110. Wu, S.N.; Wu, Y.H.; Chen, B.S.; Lo, Y.C.; Liu, Y.C. Underlying mechanism of actions of tefluthrin, a pyrethroid insecticide, on voltage-gated ion currents and on action currents in pituitary tumor (GH_3) cells and GnRH-secreting (GT1-7) neurons. *Toxicology* **2009**, *258*, 70-77. doi: 10.1016/j.tox.2009.01.009.
111. Lin, M.H.; Lin, J.F.; Yu, M.C.; Wu, S.N.; Wu, C.L.; Cho, H.Y. Characterization in Potent Modulation on Voltage-Gated Na^+ Current Exerted by Deltamethrin, a Pyrethroid Insecticide. *Int. J. Mol. Sci.* **2022**, *23*, 14733. doi: 10.3390/ijms232314733.
112. Huang, H.Y.; Huang, Y.B.; Wu, C.L.; Wu, S.N. Modulatory Impact of Tefluthrin, Telmisartan, and KB-R7943 on Voltage-Gated Na^+ Currents. *Biophysica* **2024**, *4*, 488-506. https://doi.org/10.3390/biophysica4040032.
113. Hou, S.M.; Hsia, C.W.; Tsai, C.L.; Hsia, C.H.; Jayakumar, T.; Velusamy, M.; Sheu, J.R. Modulation of human platelet activation and in vivo vascular thrombosis by columbianadin: regulation by integrin $\alpha_{IIb}\beta_3$ inside-out but not outside-in signals. *J. Biomed. Sci.* **2020**, *27*, 60. doi: 10.1186/s12929-020-0619-5.
114. Kang, J.I.; Hong, J.Y.; Choi, J.S.; Lee, S.K. Columbianadin Inhibits Cell Proliferation by Inducing Apoptosis and Necroptosis in HCT116 Colon Cancer Cells. *Biomol. Ther.* (Seoul). **2016**, *24*, 320-327. doi: 10.4062/biomolther.2015.145.
115. Köseoğlu, B.G.; Tanrikulu, S.; Sübay, R.K.; Sencer, S. Anesthesia following overfilling of a root canal sealer into the mandibular canal: a case report. *Oral Surg. Oral Med. Oral Pathol. Oral Radiol. Endod.* **2006**, *101*, 803-806.

 doi:10.20944/preprints202603.0263.v1

116. Irie, Y.; Keung, W.M. *Rhizoma acori graminei* and its active principles protect PC-12 cells from the toxic effect of amyloid-◎ peptide. *Brain Res.* **2003**, *963*, 282-289.
117. Li, J.; Liu, X.; Liu, X.; Zhou, Y.; Wang, L. Interplay between olfactory inputs and seizure regulation: Mechanisms and evidence. *Epilepsy Behav.* **2026**, *177*, 110897. doi: 10.1016/j.yebeh.2026.110897.
118. Müller, M.; Pape, H.C.; Speckmann, E.J.; Gorji, A. Effect of eugenol on spreading depression and epileptiform discharges in rat neocortical and hippocampal tissues. *Neuroscience* **2006**, *140*, 743-751.
119. Huang, C.W.; Chow, J.C.; Tsai, J.J.; Wu, S.N. Characterizing the effects of Eugenol on neuronal ionic currents and hyperexcitability. *Psychopharmacology* (Berl) **2012**, 221, 575-587. doi: 10.1007/s00213-011-2603-y.
120. Teixeira-Fonseca, J.L.; Santos-Miranda, A.; da Silva, J.B.; Marques, L.P.; Joviano-Santos, J.V.; Nunes, P.I.C.; Roman-Campos, D.; Gondim, A.N.S. Eugenol interacts with cardiac sodium channel and reduces heart excitability and arrhythmias. *Life Sci.* 2021, *282*, 119761. doi: 10.1016/j.lfs.2021.119761.
121. Yang, B.H.; Piao, Z.G.; Kim, Y.B.; Lee, C.H.; Lee, J.K.; Park, K.; Kim, J.S.; Oh, S.B. Activation of vanilloid receptor 1 (VR1) by eugenol. *J. Dent. Res.* **2003**, *82*, 781-785.
122. Chung, G.; Rhee, J.N.; Jung, S.J.; Kim, J.S.; Oh, S.B. Modulation of Cav2.3 calcium channel currents by eugenol. *J. Dent. Res.* **2008**, *87*, 137-141.
123. Huang, C.W.; Chow, J.C.; Tsai, J.J.; Wu, S.N. Characterizing the effects of Eugenol on neuronal ionic currents and hyperexcitability. *Psychopharmacology* (Berl) **2012**, *221*, 575-587. doi: 10.1007/s00213-011-2603-y.
124. Li, H.F.; Chen, S.A.; Wu, S.N. Evidence for the stimulatory effect of resveratrol on Ca^{2+}-activated K^+ current in vascular endothelial cells. *Cardiovasc. Res.* **2000**, *45*, 1035-45. doi: 10.1016/s0008-6363(99)00397-1.
125. Zhang, L.X.; Li, C.X.; Kakar, M.U.; Khan, M.S.; Wu, P.F.; Amir, R.M.; Dai, D.F.; Naveed, M.; Li, Q.Y.; Saeed, M.; Shen, J.Q.; Rajput, S.A.; Li, J.H. Resveratrol (RV): A pharmacological review and call for further research. *Biomed. Pharmacother.* **2021**, *143*, 112164. doi: 10.1016/j.biopha.2021.112164.
126. Caiati C, Jirillo E. Cellular and Molecular Bases for the Application of Polyphenols in the Prevention and Treatment of Cardiovascular Disease. *Diseases* **2025**, *13*, 221. doi: 10.3390/diseases13070221.
127. Rao, Y.L.; Ganaraja, B.; Joy, T.; Pai, M.M.; Ullal, S.D.; Murlimanju, B.V. Neuroprotective effects of resveratrol in Alzheimer's disease. *Front. Biosci.* (Elite Ed) **2020**, *12*, 139-149. doi: 10.2741/E863.
128. Kim, H.J.; Kim, I.K.; Song, W.; Lee, J.; Park, S. The synergic effect of regular exercise and resveratrol on kainate-induced oxidative stress and seizure activity in mice. *Neurochem. Res.* 2013, *38*, 117-122. doi: 10.1007/s11064-012-0897-8.
129. Almeida, E.R.; Lima-Rezende, C.A.; Schneider, S.E.; Garbinato, C.; Pedroso, J.; Decui, L.; Aguiar, G.P.S.; Müller, L.G.; Oliveira, J.V.; Siebel, A.M. Micronized Resveratrol Shows Anticonvulsant Properties in Pentylenetetrazole-Induced Seizure Model in Adult Zebrafish. *Neurochem. Res.* **2021**, *46*, 241-251. doi: 10.1007/s11064-020-03158-0.
130. Wang, Y.J.; Chan, M.H.; Chen, L.; Wu, S.N.; Chen, H.H. Resveratrol attenuates cortical neuron activity: roles of large conductance calcium-activated potassium channels and voltage-gated sodium channels. *J. Biomed. Sci.* **2016**, *23*, 47. doi: 10.1186/s12929-016-0259-y.
131. Granados-Soto, V.; Arguelles, C.F.; Ortiz, M.I. The peripheral antinociceptive effect of resveratrol is associated with activation of potassium channels. *Neuropharmacology* **2002**, *43*, 917–923.
132. Tang, C.; Wu, B.; Wu, J.; Zhang, Z.; Yu, B. Novel strategies using total gastrodin and gastrodigenin, or total gastrodigenin for quality control of *Gastrodia elata*. *Molecules* 2018, *23*, 270.
133. Liu, Y.; Gao, J.; Peng, M.; Meng, H.; Ma, H.; Cai, P.; Xu, Y.; Zhao, Q.; Si, G. A review on central nervous system effect of gastrodin. *Front. Pharmacol.* **2018**, *9*, 24.
134. Yang, C.S.; Chiu, S.C.; Liu, P.Y.; Wu, S.N.; Lai, M.C.; Huang, C.W. Gastrodin alleviates seizure severity and neuronal excitotoxicities in the rat lithium-pilocarpine model of temporal lobe epilepsy via enhancing GABAergic transmission. *J. Ethnopharmacol.* **2021**, *269*, 113751. doi: 10.1016/j.jep.2020.113751.
135. Dai, J.; Shen, H.L.; Li, J.; Zhou, Y.; Dong, Z.X.; Zhu, X.Y. Gastrodin Attenuates Neuroinflammation and Injury in Young Rats with LiCl/Pilocarpine-Induced Status Epilepticus. *Biochem. Genet.* **2025**, *63*, 5067-5082. doi: 10.1007/s10528-024-10971-7.

 doi:10.20944/preprints202603.0263.v1

136. Wang, D.; Liu, W.; Lu, M.; Xu, Q. Neuropharmacological effects of *Gastrodia elata* Blume and its active ingredients. *Front. Neurol.* **2025**, *16*, 1574277. doi: 10.3389/fneur.2025.1574277.

137. Yang, C.S.; Lai, M.C.; Liu, P.Y.; Lo, Y.C.; Huang, C.W.; Wu, S.N. Characterization of the Inhibitory Effect of Gastrodigenin and Gastrodin on M-type K^+ Currents in Pituitary Cells and Hippocampal Neurons. *Int. J. Mol. Sci.* **2019**, *21*, 117. doi: 10.3390/ijms21010117.

138. Ahmad, H.; Rajagopal, K. Pharmacology of *Pterocarpus marsupium* Roxib. *Medicinal Plant Research* **2015**, *5*, 1-6.

139. Tan, K.;, Chen, P.W.; Li, S.; Ke, T.M.; Lin, S.H.; Yang, C.C. Pterostilbene inhibits lung squamous cell carcinoma growth in vitro and in vivo by inducing S phase arrest and apoptosis. *Oncol. Lett.* **2019**, *18*, 1631-1640.

140. Yu, C.L.; Yang, S.F.; Hung, T.W.; Lin, C.L.; Hsieh, Y.H.; Chiou, H.L. Inhibition of eIF2alpha dephosphorylation accelerates pterostilbene-induced cell death in human hepatocellular carcinoma cells in an ER stress and autophagy-dependent manner. *Cell Death Dis.* **2019**, *10*, 418.

141. Zhang, T.; Li, B.; Feng, Q.; Xu, Z.; Huang, C.; Wu, H.; Chen, Z.; Hu, L.; Gao, L.; Liu, P.; Yang, G.; Zhang, H.; Lu, K.; Li, T.; Tao, Y.; Wu, X.; Shi, J.; Zhu, W. DCZ0801, a novel compound, induces cell apoptosis and cell cycle arrest via MAPK pathway in multiple myeloma. *Acta Biochim. Biophys. Sin.* (Shanghai) **2019**, *51*, 517-523.

142. So, E.C.; Gao, Z.H.; Ko, S.Y.; Wu, S.N. Characterization of Effectiveness in Concerted I_h Inhibition and $I_{K(Ca)}$ Stimulation by Pterostilbene (Trans-3,5-dimethoxy-4'-hydroxystilbene), a Stilbenoid. *Int. J. Mol. Sci.* **2020**, *21*, 357. doi: 10.3390/ijms21010357.

143. Wu, S.N.; Chern, J.H.; Shen, S.; Chen, H.H.; Hsu, Y.T.; Lee, C.C.; Chan, M.H.; Lai, M.C.; Shie, F.S. Stimulatory actions of a novel thiourea derivative on large-conductance, calcium-activated potassium channels. *J. Cell. Physiol.* **2017**, *232*, 3409-3421.

144. Sobhani, M.; Abbas-Mohammadi, M.; Ebrahimi, S.N.; Aliahmadi, A. Tracking leading anti-Candida compounds in plant samples; *Plumbago europaea*. *Iran. J. Microbiol.* **2018**, *10*, 187-193.

145. Liu, Y.; Cai, Y.; He, C.; Chen, M.; Li, H. Anticancer Properties and Pharmaceutical Applications of Plumbagin: A Review. *Am. J. Chin. Med.* **2017**, *45*, 423-441.

146. Roy, R.; Mandal, S.; Chakrabarti, J.; Saha, P.; Panda, C.K. Downregulation of Hyaluronic acid-CD44 signaling pathway in cervical cancer cell by natural polyphenols Plumbagin, Pongapin and Karanjin. *Mol. Cell. Biochem.* **2021**, *476*, 3701-3709.

147. Zhang, Q.; Zhao, S.; Zheng, W.; Fu, H.; Wu, T.; Hu, F. Plumbagin attenuated oxygen-glucose deprivation/reoxygenation-induced injury in human SH-SY5Y cells by inhibiting NOX4-derived ROS-activated NLRP3 inflammasome. *Biosci. Biotechnol. Biochem.* **2020**, *84*, 134-142.

148. Thakor, N.; Janathia, B. Plumbagin: A Potential Candidate for Future Research and Development. *Curr. Pharm. Biotechnol.* 2022, *23*, 1800-1812. doi: 10.2174/1389201023666211230113146.

149. Bhargava, S.K. Effect of testosterone replacement therapy on quantitative spermatogenesis following plumbagin treatment in immature rats. *Acta Eur. Fertil.* **1986**, *17*, 217-219.

150. Shen, A.Y.; Huang, M.H.; Teng, C.M.; Wang, J.S. Inhibition of 2-P-mercaptophenyl-1,4-naphthoquinone on human platelet function. *Life Sci.* **1999**, *65*, 45-53.

151. Huang, M.H.; Wu, S.N.; Chen, C.P.; Shen, A.Y. Inhibition of Ca^{2+}-activated and voltage-dependent K^+ currents by 2-mercaptophenyl-1,4-naphthoquinone in pituitary GH_3 cells: contribution to its antiproliferative effect. *Life Sci.* **2002**, *70*, 1185-1203.

152. Chen, L.; Cho, H.Y.; Chuang, T.H.; Ke, T.L.; Wu, S.N. The Effectiveness of Isoplumbagin and Plumbagin in Regulating Amplitude, Gating Kinetics, and Voltage-Dependent Hysteresis of *erg*-mediated K^+ Currents. *Biomedicines* **2022**, *10*, 780. doi: 10.3390/biomedicines10040780.

153. Tsao, Y.C.; Chang, Y.J.; Wang, C.H.; Chen, L. Discovery of Isoplumbagin as a Novel NQO1 Substrate and Anti-Cancer Quinone. *Int. J. Mol. Sci.* **2020**, *21*, 4378. doi: 10.3390/ijms21124378.

154. Liu, P.Y.; Chang, W.T.; Wu, S.N. Characterization of the synergistic inhibition of $I_{K(erg)}$ and $I_{K(DR)}$ by ribociclib, a cyclin-dependent kinase 4/6 inhibitor. *Int. J. Mol. Sci.* **2020**, *21*, 8078.

155. Stojilkovic, S.S.; Tabak, J.; Bertram, R. Ion channels and signaling in the pituitary gland. *Endocr. Rev.* **2010**, *31*, 845-915.

 doi:10.20944/preprints202603.0263.v1

156. Vandenberg, J.I.; Perry, M.D.; Perrin, M.J.; Mann, S.A.; Ke, Y.; Hill, A.P. hERG K^+ channels: structure, function, and clinical significance. *Physiol. Rev.* **2012**, *92*, 1393-1478.

157. Martinson, A.S.; Van Rossum, D.B.; Diatta, F.H.; Layden, M.J.; Rhodes, S.A.; Martindale, M.Q.; Jegla, T.J. Functional evolution of Erg potassium channel gating reveals an ancient origin for IKr. *Proc. Natl. Acad. Sci. U.S.A.* **2014**, *111*, 5712-5717.

158. Min, J.Y.; Lv, Y.; Mao, L.; Gong, Y.Y.; Gu, Q.; Wei, F. A rodent model of anterior ischemic optic neuropathy (AION) based on laser photoactivation of verteporfin. *BMC Ophthalmol.* **2018**, *18*, 304. doi: 10.1186/s12886-018-0937-5.

159. Iacono, P.; Toto, L.; Eliana, C.; Varano, M.; Parravano, M.C. Pharmacotherapy of central serous chorioretinopathy: review of the current treatments. *Curr. Pharm. Des.* **2019**, *24*, 4864-4873. doi: 10.2174/1381612825666190123165914.

160. Isildak, H.; Schwartz, S.G.; Flynn, H.W. Pharmacotherapy of myopic choroidal neovascularization. *Curr. Pharm. Des.* **2019**, *24*, 4853-4859. doi: 10.2174/1381612825666190124102641.

161. Tekrony, A.D.; Kelly, N.M.; Fage, B.A.; Cramb, D.T. Photobleaching kinetics of verteporfin and lemuteporfin in cells and optically trapped multilamellar vesicles using two-photon excitation. *Photochem. Photobiol.* **2011**, *87*, 853-861. doi: 10.1111/j.1751-1097.2011.00933.x.

162. Nemes, A.; Fortmann, T.; Poeschke, S.; Greve, B.; Prevedello, D.; Santacroce, A.; Stummer, W.; Senner, V.; Ewelt, C. 5-ALA fluorescence in native pituitary adenoma cell lines: resection control and basis for photodynamic therapy (PDT)? *PLoS One* **2016**, *11*, e0161364. doi: 10.1371/journal.pone.0161364.

163. Valenzeno DP, Tarr M. Calcium as a modulator of photosensitized killing of H9c2 cardiac cells. *Phtochem. Photobiol.* **2001**, *74*, 605-610. PMID: 11683041.

164. Karacorlu, M.; Karacorlu, S.; Ozdemir, H. Nonarteritic anterior ischemic optic neuropathy after photodynamic therapy for choroidal neovascularization. *Jpn. J. Ophthalmol.* **2004**, *48*, 424-426. doi: 10.1007/s10384-004-0078-7.

165. Huang, M.H.; Liu, P.Y.; Wu, S.N. Characterization of Perturbing Actions by Verteporfin, a Benzoporphyrin Photosensitizer, on Membrane Ionic Currents. *Front. Chem.* **2019**, *7*, 566. doi: 10.3389/fchem.2019.00566.

166. Gibault, F.; Corvaisier, M.; Bailly, F.; Huet, G.; Melnyk, P.; Cotelle, P. Non-photoinduced biological properties of verteporfin. *Curr. Med. Chem.* **2016**, *23*, 1171-1184. PMID: 26980565 doi : 10.2174/0929867323666160316125048.

167. Chen, Y.; Hu, Y. Photodynamic therapy for an iris metastasis from pulmonary adenocarcinoma. *Photodiagnosis Photodyn. Ther.* **2017**, *20*, 246-247. doi: 10.1016/j.pdpdt.2017.10.011.

168. Marks, P.V.; Belchetz, P.E.; Saxena, A.; Igbaseimokumo, U.; Thomson, S.; Nelson, M.; Stringer, M.R.; Holroyd, J.A.; Brown, S.B. Effect of photodynamic therapy on recurrent pituitary adenomas: clinical phase I/II trial--an early report. *Br. J. Neurosurg.* **2000**, *14*, 317-325.

169. Wu, S.N.; Wang, Y.J.; Gao, Z.H.; Liutkevičienė, R.; Rovite, V. Recent Advances in Ionic Mechanisms in Pituitary Cells: Implications for Electrophysiological and Electropharmacological Research. *J. Clin. Med.* 2025, *14*, 3117. doi: 10.3390/jcm14093117.

170. Lin, C.Y.; Gao, Z.H.; Cheung, C.W.; So, E.C.; Wu, S.N. Modulation of Voltage-Gated Na+ Channel Currents by Small Molecules: Effects on Amplitude and Gating During High-Frequency Stimulation. *Sci. Pharma.* 2025, 93, *33*. https://doi.org/10.3390/scipharm93030033.

171. Tsuchiya, H. Membrane Interactions of Phytochemicals as Their Molecular Mechanism Applicable to the Discovery of Drug Leads from Plants. *Molecules* 2015, *20*, 18923-66. doi: 10.3390/molecules201018923.